JPRS-CST-86-050

28 NOVEMBER 1986

China Report

SCIENCE AND TECHNOLOGY

FBIS FOREIGN BROADCAST INFORMATION SERVICE

NOTE

JPRS publications contain information primarily from foreign newspapers, periodicals and books, but also from news agency transmissions and broadcasts. Materials from foreign-language sources are translated; those from English-language sources are transcribed or reprinted, with the original phrasing and other characteristics retained.

Headlines, editorial reports, and material enclosed in brackets [] are supplied by JPRS. Processing indicators such as [Text] or [Excerpt] in the first line of each item, or following the last line of a brief, indicate how the original information was processed. Where no processing indicator is given, the information was summarized or extracted.

Unfamiliar names rendered phonetically or transliterated are enclosed in parentheses. Words or names preceded by a question mark and enclosed in parentheses were not clear in the original but have been supplied as appropriate in context. Other unattributed parenthetical notes within the body of an item originate with the source. Times within items are as given by source.

The contents of this publication in no way represent the policies, views or attitudes of the U.S. Government.

PROCUREMENT OF PUBLICATIONS

JPRS publications may be ordered from the National Technical Information Service, Springfield, Virginia 22161. In ordering, it is recommended that the JPRS number, title, date and author, if applicable, of publication be cited.

Current JPRS publications are announced in Government Reports Announcements issued semi-monthly by the National Technical Information Service, and are listed in the Monthly Catalog of U.S. Government Publications issued by the Superintendent of Documents, U.S. Government Printing Office, Washington, D.C. 20402.

Correspondence pertaining to matters other than procurement may be addressed to Joint Publications Research Service, 1000 North Glebe Road, Arlington, Virginia 22201.

JPRS-CST-86-050

28 NOVEMBER 1986

CHINA REPORT

SCIENCE AND TECHNOLOGY

CONTENTS

PEOPLE'S REPUBLIC OF CHINA

ABSTRACTS

/9986

NATIONAL DEVELOPMENTS

XICHANG SATELLITE LAUNCH SITE BEING UPGRADED

HK050851 Hong Kong WEN WEI PO in Chinese 4 Nov 86 p 1

[Report by contributing reporter Yang Yung-nien [2799 3057 1628]: "Construction Work To Expand the Xichang Satellite Launching Center Begins"]

[Text] In order to better meet the needs of putting our country's carrier rockets in the international markets, the Xichang Satellite Launch Center in Sichuan Province will be expanded and rebuilt. The inaugural ceremony of the expansion project was held at the launch site on 1 November.

Since the satellite launching center was built in 1984, it has successfully launched Changzheng-3 carrier rockets to send three synchronous communications satellites into outer space. Now, a number of companies in the United States, Sweden, and Britain have expressed the desire to use the Xichang launching center to launch their satellites.

The project of the Xichang launching center started in the mid 1970's. The site enjoys such favorable natural conditions such as being located at a low latitude, a narrow yearly temperature difference, and a short wet season. The testing, launching, surveying, and controlling equipment in the center, as well as the Changzheng rockets and satellites, are all designed and produced by China herself.

In addition, the fuel used by the third stage of the Changzheng-3 rockets launched by the Xichang center is liquid hydrogen and oxygen newly developed by the research organizations. Such liquid fuel releases high energy at a comparatively low temperature. At present, only the United States, France, and China have mastered the technology of producing such sophisticated fuel. The Soviet Union is still in the testing stage.

/9716
CSO: 4008/12

NATIONAL DEVELOPMENTS

STRATEGIC SIGNIFICANCE OF 'SPARK PLAN' DISCUSSED

Tianjin KEXUEXUE YU KEXUE JISHU GUANLI [SCIENCE OF SCIENCE AND MANAGEMENT OF S& T] in Chinese No 3, 1986 p 1

[Article by Shen Zongqi [3088 1350 3825], Tianjin Science and Technology Commission: "An Important Strategic Change"]

[Text] The Technological Development Plan for promoting the vitalization of local economies (abbreviated, "Sparks Plan"), which was passed by the CPC Central Committee and the State Council, and entrusted by these bodies to the State Scientific and Technological Commission for implementation is a strategic plan of historical significance that will restructure Chinese agriculture and enable us to arm town and township enterprises with science and technology.

The Spark Plan will erect a golden bridge joining S&T cadres and hundreds of millions of peasants and become a link orienting S&T and educational departments toward economic development and the vitalization of local economies. The plan emphasizes local, and town and township enterprises and thus embraces both the basic direction for the vitalization of China's rural and town and township economies as well as the general path for future enterprise development. As a fundamental long-term policy, the Spark Plan must proceed along a path which has Chinese characteristics.

When localities draw up their own specific Spark Plan they must proceed in a planned and organized manner under the guidance of the State S&T Commission and other central ministries and commissions. Local plans should proceed from local strategic development objectives, provide for systemic development and strive to make the life of the masses more convenient and to promote transfers of foreign technology to China; transfers of coastal technology to the interior; transfers of technology developed by central departments, research institutes and institutions of higher learning to localities; integration among localities; and demonstration and extension. Projects provided in the Spark Plan should not compete with big industry for raw materials and markets but rather should promote cooperation and coordination through division of labor and comparative advantage and thereby allow localities to exploit their own technological strengths, to promote rational and comprehensive use of resources, to engage in more sophisticated types of production, to rapidly

transform these strengths into market advantage and to make these strengths an important pillar buttressing local technological and economic development.

Local enterprises, especially those run by towns and townships, now "thirst" for technology and capable personnel and are in great need of concrete guidance and support from the S&T front. Thus S & T circles throughout the nation should take up this heavy historical task and work through the Spark Plan to send S&T to localities and villages in a planned and organized fashion and on a big scale, so as to enable local and rural economies to advance more healthily. Thus we must attach much, much more importance to the scientificalness, the technical applicability and the technical advancement of, and the demonstration effect of extension work involved in, Spark Plan projects and employ S&T to implant new embryos in local enterprises, accelerate modernization of local enterprises, enable villages to free themselves from the habits associated with the mode of production of the natural economy, guide localities toward the factory mode of production and thus vitalize local and rural economies.

In implementing the Spark Plan, we must note its layered structure, the web-like way in which it is to be organized and its ladder-like, step-by-step approach to transfers of skilled personnel, technology and management.

Implementation of the Spark Plan marks the beginning of a new stage in in which S&T development planning is to be more closely linked to production and oriented toward economic development. The Spark Plan will eliminate exclusive reliance on physical labor, attract more attention to intellectual development and lead to greater efforts to create a new, mighty army of labor that is hundreds of millions strong. The plan will forcefully spur the rural economy to shift from a labor-intensive to a capital-intensive track and enterprises to shift from an internally to an externally oriented track and thus will strengthen people's conviction that "the restructuring of the agricultural mix must be effected by using S&T to develop town and township enterprises." Through continuous exploration and practice, the plan will surely forge a unique path that will help reduce the disparity between city and countryside by enabling people to leave the soil but not the village and to enter the factory but not the city.

The Spark Plan accords with actual conditions in China, bears Chinese characteristics and, when implemented, will comprise an important part of the reform of the S&T and educational administrative systems. Thus the need to strengthen scientific management and macroscopic control has become very important. The broad masses of scientific workers must apply both modern management and the general laws of science in formulating and administering the SP; integrate science, technology, education, industry, agriculture and trade; and coordinate S&T development with economic and social development. The new realm created by the Spark Plan bears the seeds of new breakthroughs in science and modern management.

Implementation of the Spark Plan constitutes important preparatory work for China's great undertaking, the four modernizations, will stimulate tremendous changes in the modes of production and way of life of China's 800 million peasants and will play an equally significant role in urban development. Thus only a strategic shift on the S&T battle front can enable the sparks of the technological development plan to ignite the whole prairie.

12431
CSO: 4008/2101

NATIONAL DEVELOPMENTS

ORGANIZATIONAL PROBLEMS OF RESEARCH INSTITUTES ANALYZED

Tianjin KEXUEXUE YU KEXUE JISHU GUANLI [SCIENCE OF SCIENCE AND MANAGEMENT OF S& T] in Chinese No 3 1986 pp 7-10

[Article by Yang Guangji [2799 1639 3444], Northwest Botany Institute: "Components, Structures, Mechanisms: The Organizational Problems of Research Institutes"]

[Text] I. Components

The organizational components of research institutes consist of three levels: disciplines, specialized skills and the functions of these two elements; human, financial, material and informational resources; and various managerial functions.

A. Why Do We Treat Disciplines, Specialized Skills and the Functions of These Two Elements as a Level? Intellectual Production Differs from Material Production, and the Essential Characteristic of Intellectual Production Is That Knowledge Produces Knowledge. Thus the Study of Intellectual Components Forms the First Level in Analyzing Scientific Productive Forces.

We must analyze the logical structure internal to disciplines, to specialized skills and to the functions of these elements, understand the organic relationships among these three components, actively promote the rationalization of their logical structure, consciously manipulate their organic relationships and thereby achieve our objective of increasing scientific capability. In general, for disciplines, differentiation and integration are the most important processes; for skills, specialization and coordination are crucial; and for functions the issue is one of stability and change.

1. There is a general law concerning the differentiation and integration of disciplines, and that is that synthesis occurs first, then comes integration and finally there is differentiation. At first, different types of specialists work together using existing, traditional knowledge and methodologies to complete a given scientific task. If problems are resolved through traditional knowledge and methodologies alone, the work does not go beyond the stage of synthesis. But if in joint research projects different types of knowledge and methodologies are assimilated (or converge) to produce

new knowledge or methodologies, then integration has occurred, for integration is the product of partial qualitative change. Then, as scientific intercourse increases, that is, as knowledge and methodology are increasingly integrated, new branches appear, which process is called differentiation. Only at this stage does a new field acquire the distinctive features defining that field as a discipline, thereby completing the process.

Two factors are interrelated with this integration-differentiation process: research projects that give momentum to, and nodular structures which provide the organizational framework of, the process. Without the interaction and organic relationships that occur in research projects, there would be no contact between disciplines, none of the partial qualitative change that is involved in the transition from integration to differentiation, no generation of internal cohesion and no improvement in organizational efficiency. This law by all means should be employed in microscopic management. Contacts among relevant disciplines invariably occurs as multidisciplinary intercourse among a number of research groups or institutes, and the groups, offices and institutes that have the most ties become nodes in this web of relationships. All interaction between groups, offices and institutes, whether the ties are established through research projects or communication among individual scientists, should be vigorously supported. Otherwise, the new sprouts of association will be squashed.

We must consciously organize research institutes into integral wholes. The way to determine the extent of institute integration is to examine the ratios of the number of inter-group and inter-office projects to the total number of projects undertaken and the ratio of the total amount of results produced by multidisciplinary projects to the total number of research results produced in the entire unit. The greater the ratio, the more formal the organization. We can also measure institute integration by using interviews to determine the degree of individual interaction, which represents spontaneous, informal organization, facilitates project planning and reflects the need for exploratory projects.

2. With respect to the specialization of and coordinated interaction among skills, there is also a law that can generally be followed, and that is that the development of science and specialized skills is a two-way street along which the two elements combine and reseparate as science becomes skill and skill, science and as the two processes affect each other. This law is manifested in the areas of personnel and equipment. In terms of personnel, the law works as follows: Either 1) scientists serve also as laboratory specialists, and many scientists have mastered multiple specialized skills, or 2) scientists and laboratory skills are separated, in which case two discrete roles emerge--theoretical scientists and empirical scientists. In the area of equipment, the law works as follows: Either 1) instruments and researchers are brought together, or 2) instruments are separated from researchers, in which case management by specialized departments is required.

We may be able to solve the problem better within a few years if, in management work, we use the principles of dissipation, put the law of value to use, liberalize the management system, and draw up technical development plans, beginning by reordering specialized skills within institutes. And for

an individual institute, in the area of technical development alone, the formula: specialization + coordinated interaction + management system = organizational efficiency will create impressive intangible scientific potential and concrete economic results.

3. With respect to functional stability and change, there are first of all functions separately produced by disciplines and specialized skills and then there are functions produced through the interaction among disciplines, among skills and between disciplines and skills. Stability is required for the first type of functions, and change is needed for the second. We need consistency to counter great fluctuation; change cannot be effected flexibly if stability is not assured.

B. The Second Level of Research Institute Organizational Components Consists of Human, Financial, Material and Informational Resources. For These Elements, Balanced Development and Rational Use Are Required

1. Human resources are first of all researchers and technicians and then management and security personnel. We shall focus our discussion on researchers and technicians, primarily analyzing their expertise, and functional and age distributions.

In an institute, it is most essential that the mix of researcher expertise correspond to the nature of the work conducted by the institute. Insufficient depth or breadth in researcher expertise invariably will affect research quality.

When analyzing the functional mix of researchers, we must select the most basic unit of scientific aggregation (the group or office) as our focus of investigation and then choose the most general functions affecting the productive forces of scientific groups. These functions include academic influence, organizational work and scientific intercourse and are personified in the roles of leaders, organizers and communicators. We distinguish first-, second-, and third-level leaders as well as nonleaders according to the amount of academic influence people have within the group: large, medium, small or none. We can also divide people into first- and second-level organizers as well as nonorganizers according to organizational ability. And we can categorize people as first-, second- and third-level communicators and noncommunicators in terms of people's ability to associate across office and across institute. In individual researcher performance, these three capabilities and four levels will combine to form many different researcher types. Of course, the most ideal researcher would be one who combines, at high levels, leader, organizer and communicator roles. In general, basic scientific aggregations (whether offices or groups, these must be integral wholes) will achieve greater efficiency if top posts are filled by persons combining at least two roles--leaders and organizers--and if these people are assisted by persons combining all three roles--leaders, communicators and organizers.

There is also the matter of age distribution. People are most creative at the age of 35, give or take 10 years. In response to a draft proposal of UNESCO, the Ukrainian Research Institute studied 200 research groups at 10 scientific institutes and 3 departmental institutes and concluded that it is proper for

young and old researchers to work together and that old scholars (above the age of 50) should not exceed 20 percent of the total number of people employed in the research group.

2. As for financial, material and informational resources, we can only state here that, in the case of financial resources, revenues should be broadened, expenditures should be reduced and funds should be used rationally. Yet the present ratios between administrative expenses and research costs and between expenditures on equipment and personnel demonstrate that funds have not been put to rational use.

C. The Second Level in Institute Organizational Components Consists of Managerial Functions. The Question of Whether or Not To Establish a Given Managerial Function Is Determined by Such Factors as the Size of the Institute, the Nature of Its Research, Government Policy and the Form of Management Employed by the Institute. In Dealing with This Issue, We Should Determine the Laws of the Development of Institute Management by Examining Conditions in Many Institutes and Should Not Arbitrarily Insist on the Creation of Certain Numbers of Managerial Functions

II. Structures

What sort of criteria should we use in designing institute organizational charts? For the most part, we should take four areas into consideration: the components of the organization, the tasks the organization will assume, the form of management the organization employs and general principles of administrative management.

A. Select Structural Forms on the Basis of Results Obtained through Analysis of the Attributes of Organizational Components

When we analyze actual conditions within the first level of institute organizational components, that is, among disciplines, skills and their related functions, we discover that the actual levels of development of these elements differ and that the elements characteristically change through random interaction. These facts provide the criteria for selecting structural form. For random interaction, as an attribute, by definition generates a network structure, and if this attribute is not well developed, the structure of the organization will not take on the clear shape of a network but rather will appear as the dots and lines of a flow chart or the branches and trunk of the goal tree. Still, networks are the ultimate form in such development, for dots and lines and branches and trunks represent networks in incomplete form.

As for the second level of institute organizational components, that is, among human, financial, material and informational resources, we certainly should adopt a full variety of structural forms to deal with human resources and employ whatever form best suits the specific scientific unit in question. In dealing with financial and material resources, we should act courageously, flexibly and imaginatively and take resource availability into account. When financial resources are abundant, for example, we, for the sake of convenience, may employ the systems structure embodied in the goal tree and focus on large systems, subsystems and sub-sub systems. But to exploit

financial potential and to strengthen intensification, a network structure should be selected.

B. The Second Criterion for the Selection of Structural Form Is the Tasks the Organization Will Perform

1. Using the task systems chart--the branch and trunk structure. In determining organizational structure, leaders first of all want to take into consideration the long- and short-term tasks their organization will perform, and thus some leaders prefer to start by drawing up task charts for their institutes, breaking general objectives into first- and second-degree goals, and then to design organizational structure on the basis of task-assignment systems charts. This kind of structure can be broken down by scientific discipline or by research stage but always takes the shape of the goal tree, with its trunk and branches, and seeks to provide for self-adjustment at each systems level.

2. Using the activity structure chart--mixed forms. If we were to propose a different principle, namely, "let's use activity structure charts to represent organizational structure," we would discover that the systems-theory based goal tree discussed above does not reflect the activities among branches very clearly. Thus would arise many types of mixed structures, one of which is the essential-objectives form, another is the project form and still another is the matrix form. These forms differ in the following ways. The essential-objectives form provides for no management body or independent superiors for project groups but rather for ad hoc task groups drawn from permanent scientific-discipline offices according to need as reflected in the essential objectives of the research project. The project form establishes both administrative superiors and an administrative body that is responsible for linking projects with disciplines, and the project office in this form combines academic and administrative functions under one roof. In the matrix form, the project group has superiors but no specialized administrative body, and the responsible remembers of the group serve only in academic functions and are powerless with respect to personnel and administrative affairs. These three forms, however, do share a common feature, in that they tack horizontal frameworks onto permanent vertical structures so as to give formal organizational expression to relationships among subsystems, and thus all three structures are called mixed forms.

3. Using the structures internal to science and technology--networks. If we visualize the integration and differentiation of science and technology, the specialization and coordination of skills and the stability and change in functions in three-dimensional space, we invariably discover that the relationship among these elements and their processes forms a three-dimensional network. Would it be appropriate to design organizational structures in accordance with the actual level of structural development in three dimensional space, that is, to the actual level of development of the three elements and their processes cited above in a real research institute? I should say that the network structure thus obtained would be the best form available, but of course this structure would represent a static and isolated picture. If we take into account the effects of constant external and internal change, we have to introduce a new concept, dissipation.

4. The dissipation structure of microscopic management--a kind of world view. The formula for the way in which the reciprocal effects of the dissipation structure operate reads: Function <==> structure <==> fluctuation.

If we adopt this principle and formula as a sort of world view to examine the organizational structure of research institutes, we discover that the branch-trunk and network structures and the intermediary mixed forms discussed above appear one-sided when incorporated into this formula. If we employ the principles of the dissipation structure as our guiding ideology and consciously use the dissipation formula to readjust organizational structure, we will certainly obtain a network structure that changes randomly and is very flexible. (Naturally, it fits nicely with the principle if we call this form a dissipation structure). This may prove a proper course to follow as we explore organizational structures.

C. The Form of Management Employed by Research Institutes Affects Organizational Structure

The systems--operations, entrepreneurial and the intermediary semi-operations, semi-entrepreneurial--and the types--closed, open and the intermediary semi-open--of management that are employed greatly influence the selection of and change in organizational structure.

1. The goal-tree structure of closed operations management systems. The principal feature of this system is that funds are appropriated by, employees are provided by, and output is remitted to superior agencies. This system invariably leads to eating out of the same big pot, because under this system management personnel naturally choose the branch-trunk goal-tree structure and seek to make the best use of system self-adjustment. Thus sub-systems, large or small, each try to become complete unto themselves.

2. The network structure of open entrepreneurial management systems. The most important feature of this system is that units raise or earn their own funds, hire their own employees and sell their output themselves. This system naturally smashes that old big pot, and when research institutes are opened up and liberalized scientific and technical activities are transformed into socialized behavior.

3. The mixed structure of semi-entrepreneurial, semi-open management systems. Under the state's policy of permitting different types of managerial forms to different types of activities, scientific units that serve society may obtain from the state the funds needed for the tasks they are assigned, units engaged in basic research can apply for scientific fund grants and units engaged in applied or developmental research can obtain loans or use the contract system to obtain needed funding from end users. Conditions vary greatly within many institutes, so many types of mixed structures naturally will be employed with this type of management system.

4. Employing the theories of the dissipation structure to observe, understand and consciously transform the organizational structure of research institutes. There are three basic prerequisites for the emergence of dissipation

structures: The system must be open and liberalized, the system must be in a state of great disequilibrium and the development process must be nonlinear. In the past, under the influence of the operations system, we employed closed management in institutes and research offices and, though we did have an exchange of academic ideas, did not exchange enough funds, skilled personnel, technology and equipment with the social sciences and with productive activities, and there were great imbalances among such key organizational elements as disciplines, skills and their functions; human, financial, material and informational resources; and managerial functions. This situation is called a state of great disequilibrium (though many institutes were in a state of near equilibrium). We can imagine how greatly liberalized institutes and research offices became in terms of disciplines, skills, personnel, equipment, funds, projects and the like when these units were opened up and reformed. As the economic and scientific-technological administrative systems have changed and as the relationships between commodities and money have been used to carry out market adjustment, institutes and research offices have sought to engage in greater exchanges with the outside and ultimately have experienced the following process: "In exchanging materials and effort with the outside, an open system in a state of great disequilibrium leaped from a condition of disorder to a state of order in terms of time, space and function." Or, we might say, institutes and research offices are entering a state of greater organization, that of the dissipation structure.

III. Mechanisms

A. Planning Mechanisms

1. Choosing projects and forming research groups on the basis of available personnel. We must design projects according to available personnel, planning should be flexible and research work should be broken down into smaller parts. The selection of organizational structures should be based on the academic and administrative abilities of the leaders of scientific disciplines. Creative people often are not suited to the normal patterns of organizational activity, so we should grant these people more independence and freedom, assign them tasks better geared to their personalities and abilities and challenge their competitiveness. Only in this way can we improve organizational efficiency. When undertaking broad multidisciplinary projects, we may adopt 3-dimensional structures, and we must employ the principles of the goal tree and break projects down into small parts, using planning to coordinate the entire project.

2. We should make the wide application of results a criterion for project selection. The dual nature of research projects, namely, in the way they both increase knowledge and yield practical uses, affects the direction in which the results they produce are applied. That is to say, those results might be used in a theoretical or a methodological direction, a scientific or a practical direction or as a skill or a production technique or process. Naturally, projects that produce the widest impact are the most important. So when considering organizational structures, we should consciously try to guide project selection toward broader applicability.

3. Other criteria that planning work should take into consideration are discipline stability, directional variability and carrier variety. Thus planning and organizational structures must be flexible so that the latter can adapt.

B. Economic Mechanisms

1. First we must establish external and internal commodity-money relationships. In the past, under the influence of the operations system of management, units ate out of the state's big pot and individuals ate out of units' big pots, and what we based our work on was morality and justice. But in science--except for theories, laws, and formulas and other things that represent deeper understanding of natural laws--new technology, new processes, new materials and new products all can become commodities, and various testing techniques, appraisal analyses, consultation, training and other forms of technology and intellectual services can be commercialized. Commercialization (including commercialization of labor services) has been accomplished very rapidly in institute external relations, but the concept has not been established internally, because many people oppose the idea due to conservatism and force of habit. Only internal commercialization can thoroughly smash the big pot and radically change the form of management which institutes adopt.

2. We must resolve a series of policy issues related to economic mechanisms. Economic mechanisms have their own main components such as planning, capital, prices, profits, wages, funds, contracts and the like. There are principles guiding, and limits affecting the formation of these components, and these principles and limits are rooted, in turn, in the law of value.

In planning work, for example, in the past there was planning only for research projects, including allocating funds, guaranteeing proper conditions and regulating personnel organization. Now we have added production and marketing planning (an expansion of earlier dissemination and product changeover planning), labor service planning, planning for increased earnings of foreign exchange, fiscal planning based on profits (an expansion of earlier fiscal planning) and the like. Yet even in project planning, we still have to introduce the concepts of commodities and markets.

In the area of institute funding, for another example, the most important economic mechanism is the sources and means of obtaining funds, and many countries specially formulate and constantly readjust their funding policies. China now has established a science fund system for basic and applied basic research, a system of loan grants for development institutes and a system of funding projects assigned to scientific agencies that provide public service. These policies can certainly be introduced inside of institutes, but naturally we would have to adopt appropriate complementary measures, for example, making the project group the basic unit of accounting, establishing cost accounting systems, devising a variety of channels and forms for project funding, setting up price systems within institutes and the like. If these things are properly handled, we can greatly enhance institute vitality and fully develop organizational efficiency.

3. The problems involved in separating ownership and operational authority. Ownership must be gathered upward, and operational authority must be transferred downward so that we can assure vitality and prevent chaos.

4. Establish accounting systems.

5. Establish evaluation-incentive systems.

The above represent most of the major, but not all, economic mechanisms. When designing economic management methods for a unit, we must make very certain that our plans are complete, for incompleteness is a key cause of failure. We must also make sure that our work meshes with state policy, otherwise our work cannot be successful.

C. Administrative Mechanisms

1. Supple administrative systems and dynamic management. The above discussion can be summarized in one phrase--establishing flexible administrative systems--and it would be ideal if we can consciously add dynamic management to such systems. Dynamic management means abiding by the objective and actual processes and laws of motion in scientific and technological activities, taking actual historical conditions into account and readjusting personnel, equipment, funds, information, the organizational structures of research offices and groups, and the like so as to make the best use of personnel and material and to prevent useless, inefficient waste.

2. We must use certain advanced managerial techniques, for example, project flow charts based on operations theory, systems-theory based program-goal management, psychology-based goal management and project management techniques that call for prompt organizational readjustment as research progresses. There are also a number of methodological problems relating to the evaluation of plans, results, management and potential that, if properly resolved, can improve organizational efficiency.

3. We must establish democratic and independent management systems.

12431
CSO: 4008/2101

NATIONAL DEVELOPMENTS

THIRTY YEARS OF CHINESE SPACE ENDEAVORS (CONCLUSION)

Beijing HANGTIAN [SPACEFLIGHT] in Chinese No 4, 27 Jul 86 pp 2-4

[Article by Li Chenglong [7812 2052 7893]; for Parts I and II of this series see JPRS-CST-86-038, China Report Science and Technology, 18 Sep 86, pp 19-27]

[Text] Launching of the First Satellite

On 1 April 1970, a special train carrying two "East Is Red"-1 satellites and a Long March-1 carrier rocket reached the Jiu Quan Launch Center in northwest China. On the afternoon of 2 April, Premier Zhou Enlai called a meeting in the People's Great Hall to monitor the progress of the launch operation. On the evening of 14 April, when field tests of the satellites and the carrier rocket had been completed, Premier Zhou and other officials received another report from Qian Xuesen in the People's Great Hall. Shortly after 10 pm on 16 April, Premier Zhou telephoned the National Defense Science Commission, giving his approval to transfer the satellites and carrier rocket to the launch complex.

On the morning of 24 April it was sunny and calm at the launch site. After both stages of the rocket were filled with propellant, the 8-hour countdown was started. At 3:50 pm, a telephone message from Premier Zhou Enlai was received: "Chairman Mao Zedong has approved this launch, and he is sending a personal message of encouragement to everyone, hoping they will put forth their best efforts to make this launch a success." When this directive reached the launch site, the morale of the launch crew was greatly elevated, and they vowed to succeed with their mission.

The launch time was set at 9:35 pm. Although the sky was coverd with low clouds, a command was issued to start the 30-minute countdown. Workers at the launch tower and on the launch field were ordered to assemble at a designated location. Shortly after 9 pm, the cloud cover began to break up and twinkling stars peaked through the clouds, as if greeting China's first satellite. Premier Zhou Enlai's words of advice were on everyone's mind: "The key to success is that one must be accurate, calm, steady and very cautious in one's work."

Time was ticking away, and everything was quiet at the launch site. Then came the commands: "One-minute countdown, "engage," "ignition"! As soon as the

ignition button was pushed, orange flames burst from the engines, and blocks of ice at the bottom of the launch tower were blown across a distance of 400-500 meters by the strong jet stream. At 9:35, the rocket lifted off the launch pad in a deafening roar; first it rose slowly, and then accelerated into the sky.

At 9:48, the satellite was separated from the rocket and inserted into orbit. Spontaneously, people burst out in loud cheers; some were so overwhelmed with joy that their eyes were filled with tears. On the launch field, a celebration was organized. Director Qian Xuesen, officer of the launch site, and a representative of the test team each gave an emotional speech, congratulating everyone for the successful launch of China's first satellite.

At 6 pm on 25 April, XINHUA was authorized to make the following announcement to the world: "On 24 April 1970, China successfully launched its first satellite; the satellite orbit has a perigee of 439 km, apogee of 2,384 km, inclination of 68.5 deg, and a period of 114 minutes. The satellite weighs 173 kg, and is broadcasting the song 'East is Red' on the frequency of 20.009 MHz."

Within a few seconds after this new bulletin was released, the City of Beijing was completely lit up; the sounds of gongs and drums could be heard everywhere, and a parade was formed with marching bands, banners and firecrackers, celebrating this joyful occasion of the 1970's. A number of vans traveled through the city streets to distribute leaflets reporting the goods news; everywhere they stopped, hundreds of people gathered to find out the latest information.

When the news was announced by the People's Central Broadcasting Station, the whole country celebrated. People in towns and villages all gathered around their radios and PA systems to listen to the "East Is Red" song rebroadcast by the station. When the satellite passed over the Hong Kong area, groups of local residents, young and old, went to the hill tops and beaches carrying their radios, compasses, and telescopes to look for the passing satellite in the northwestern sky.

The orbiting "East Is Red"-1 satellite added new glamour to the first international labor day--"May Festival"--of the 1970's. In the Tian An Meng Tower, Chairman Mao Zedong, Premier Zhou Enlai and other Chinese leaders greeted many representatives who participated in the development and launch of China's first satellite to express their appreciation and encouragement for the entire aerospace team.

After the successful launch of China's first satellite, many government leaders as well as private groups and individuals from friendly countries sent telegrams and letters to express their warm congratulations on China's new achievement. Experts generally agreed that the successful injection of a satellite into orbit proved that China had developed not only advanced rocket technology but also the technical capability to build large rockets.

After the "East Is Red"-1 was inserted into orbit, tests of the power system and the instrument systems showed that everything was functioning normally, and their performance met the desired specifications. In fact the operating life of all the instruments far exceeded the design requirements. The "East Is Red" sound equipment and the short-wave transmitter worked continuously for 28 days, producing a large volume of telemetry engineering data which can be used as the basis for future satellite design and development.

Retrievable Remote Sensing Satellite

China's first retrievable spacecraft was a remote sensing satellite weighing approximately 1,800 kg and in a typical orbit with a perigee of 173 km, apogee of 493 km, period of 91 minutes and inclination of 59.5 deg.

The satellite remained in orbit for 3 days, and returned to earth on 29 November 1975, bringing back the expected data collected by the remote sensors. But there were some problems with the retrieval process: for example, during the re-entry process, the skirt section of the return module and part of the electric cables and instruments were damanged by heat, and there was a large error in the predicted impact point. These problems were primarily attributed to improper design. To correct this problem, technical personnel and officers of the Institute of Aerospace Technology redesigned the satellite, and built a new spacecraft that met the required specifications; they worked around the clock, ignoring the danger of aftershocks of the Tang Shan earthquake, in order to complete the assembly and tests on schedule. In October 1976, during the festivities celebrating the downfall of the "gang of four," another of China's retrievable satellites and its carrier rocket reached the Jiu Quan launch site.

At 12:22, 7 December, the commander issued a command: "Swing the crank rod," but the crank rod failed to move. Responding to this command, three crew members rushed out of the bunker and ran toward the launch tower tens of meters away. As electricity to the elevator had been cut off, they ran up the ladder to reach the top of the launch tower 30 meters above the ground, and swung the crank rod by hand; then they quickly ran back to the bunker. The total elapsed time was only 5 minutes, thus the satellite was able to lift off without violating the "optimum launch window."

Once the satellite was injected into orbit, tracking of the satellite was initiated by personnel at the Hui Nang tracking and control center, who worked continuously for 3 days and nights. On 10 December, when the satellite was in its 47th orbit, a command was issued from the control station to the spacecraft to begin attitude adjustment. Then, an unlock command was issued, and the instrument module was disengaged from the return module. At the same time, the timing control device inside the return module was started, and proceeded to issue a sequence of commands: spin rocket ignition, braking rocket ignition, despin rocket ignition, and switch on the retrievable beacon. Following these commands, the return module headed toward the earth along a predetermined trajectory. Then, the timing control device issued another set of commands: ejection of the base cover and the braking rocket shell,

ejection of the guide chute, separation of the speed-reduction chute, and release the main chute.

The satellite recovery site in Sichuan Province was busy with activities. Five ultra-shortwave direction-finding vehicles were placed in position the day before. Four helicopters equipped with direction-finding compasses lifted off an hour before the scheduled impact time and was hovering above their assigned locations waiting for orders. A ground search team equipped with mediumwave direction-finding devices also took up their position. On the huge table inside the recovery command center was a map of the region with markings of the return trajectory; reports from the individual tracking stations were continually being monitored and broadcast through the PA system.

At about noon, a black dot appeared in the northwest part of the sky approaching the impact region accompanied by a rumbling sound. Then the black dot separated into two; one of them (the heat shield) dropped quickly and landed beside a highway, the other black dot (the return module), with a parachute trailing behind, descended slowly and finally landed in a cabbage field on a hillside. Three minutes later, a helicopter landed on a hilltop about 100 meters away; the helicopter crew and local militia rushed to the impact point and set up security measures. A short time later, all the recovery crew arrived at the site either by helicopter or by vehicle. Inspection of the return module showed that it was completely intact; not even a single screw was missing.

Scientific Experiment Satellite

A spacecraft traveling through space may suffer damage from charged particles, proton streams from the sun, shortwave radiation, ultra-violet radiation, X-rays, small meteors, and cosmic noise. The high-altitude rarefied atmosphere is the major factor affecting the orbit and life of the spacecraft. The structure of the ionosphere also affects the mode of propagation and the performance of satellite communication. Therefore, measurements of these phenomena would clearly be of scientific value. Furthermore, as the number of space missions increases, it is necessary to launch experimental satellites in order to facilitate the development of new technologies such as advanced power supply systems, advanced attitude control and orbit control systems, antenna systems, temperature control systems and new light-weight materials.

The Chinese "P" series satellites were designed to carry out the missions of exploring space science and conducting experiments for developing new aerospace technologies. The P-1 satellite was launched into orbit on 3 March 1977; it had a design life of 1 year, but the actual life was 8 years--it remained in orbit until 11 June 1979. As part of the P-1 mission, tests were conducted to determine the performance of solar battery power supply system, active/passive temperature control system, radio circuits, and long-life telemetry equipment; measurements were also made of space environment parameters such as high-altitude magnetic field, X-rays, cosmic rays, and thermal flux.

In the summer of 1977, the concept of a carrier rocket with multiple payloads was proposed. Successful implementation of this concept requires: a) a high-thrust carrier rocket; and b) a stable and reliable satellite separation procedure. Since the Fengbao-1 [Tempest-1] carrier rocket has a payload capability of over 1 ton, and has successfully completed many stage separations in the past, it was decided to use it as the carrier rocket for launching three "P" satellites: the P-2, the P-2A, and the P-2B.

The P-2 satellite incorporated many new technologies such as solar panel power supply, spin stabilization, sun sensor attitude determination, magnetic core storage, time-delay telemetry, ultra-shortwave integrated tracking and telemetry system, and passive/active temperature control.

By November 1980, all the systems and instrumenmts for the P-2 and P-2A satellites had been completed and delivered. Vice Premier Zhang Aiping, who had a great deal of interest in this project, requested that the status of technology development be frozen and the test team remain intact. In August 1981, the research personnel arrived at the Jiu Quan launch site after three quality inspections of all systems, and joined forces with the launch crew to carry out this multiple payload launch operation.

The launch time was determined based on considerations of several different requirements. For the P-2 satellite, the best launch time from the point of view of capturing the sun upon injection was between 5:20 and 14:00; from the point of view of best opportunities for observation by the ground station, the best launch time was between 4:30 and 5:30. For the P-2A satellite, which was tracked optically, the requirement was that at the time of injection, the sun should be below the horizon of the local tracking station while the satellite was still being illuminated by the sun; hence the best launch time was between 5:00 and 6:30. Based on these considerations, the overall optimum launch time was between 5:20 and 5:30.

At 5:28:40 on the morning of 20 September 1981, the Fengbao-1 carrier rocket lifted off with the three payloads: P-2, P2-A, and P-2B; 7 seconds later, it made a turn heading toward the southeast, and 3 minutes later it disappeared from view. At 7 minutes 20 seconds after lift-off, P-2A and P-2B separated from the carrier rocket, and 3 seconds later P-2 also separated; all three satellites were placed into orbits which deviated very little from their designated orbits.

The successful launch of the multiple payload rocket indicated that China's aerospace technology had taken another step forward.

Geostationary Communications Satellite

On 28 March 1984, an experimental communications satellite and its carrier rocket were transported to the launch site; the launch date was scheduled for 8 April. On that afternoon, the launch field was covered with heavy dark clouds; however, the weather department and a private 70-year-old forecaster predicted there would be no rain at launch time. Sure enough, that evening

the sky cleared up and was decorated with stars. At 19:20, a huge column of orange flame lifted the rocket off the launch pad toward the sky. At 19:40, the third stage of the carrier rocket was accurately placed into orbit, and the satellite separated from the rocket without difficulty. After the satellite was spun up to 37 rpm, it began its journey along an elliptical transfer orbit.

The launch and positioning of a communications satellite is very complicated process. Accurate injection into the elliptical transfer orbit is only the first step, and the flight time along the transfer orbit is only 20 minutes. Under ideal conditions, it would take at least 37 hours traveling along the transfer orbit, followed by three attitude control maneuvers, two transfer maneuvers, and one orbit change maneuver before the satellite can be placed in a pseudo-geostationary orbit. Under abnormal conditions, it would take at least 4 days. The information collected by the satellite and the control commands sent to the satellite are transmitted via radio signals. Therefore, accurate positioning of the satellite requires tracking and monitoring the satellite from the elliptical transfer orbit to the pseudo geostationary orbit.

Three hours before the satellite reached the apogee on its second orbit, commands were sent from the Hui Nang ground station and the Min Xi ground station to adjust the attitude of the apogee motor to prepare for firing. At 8:47 on 10 April, a remote control command was issued to fire the apogee motor, and the satellite was accurately placed into a pseudo-geostationary orbit. Some time later, other commands were issued to change the satellite's attitude so its axis became normal to the orbit plane. Then the satellite began drifting toward the designated longitude at a predetermined drift rate.

During the drift phase, there were indications of unstable fluctuations in the temperature and voltage of the battery; the sharp rise in temperature might cause damage to the battery or even total failure of the satellite. Li Feng and Huang Caiyong proposed to stop the temperature rise by changing the attitude of the spacecraft. However, this would be a severe test of the attitude control system because such attitude maneuver exceeded the design margin of the hardware; if the maneuver failed, the satellite would die prematurely. Nevertheless, the test crew proceeded to execute more than 10 accurate but bold attitude maneuvers, and eventually overcame the problem of battery overheating.

At 18:27:57 on 16 April, the satellite was successfully positioned at 125° east longitude above the equator. The despin unit on the satellite was activated so that the directional antenna would be pointing toward the earth; also, steps were taken to prepare the on-board transponder for communications tests.

The Chinese communications satellite was 3.1 m in height and 2.1 m in diameter; its lift-off weight was 900 kg, its orbit weight was 420 kg, and its orbit period was 24 hours. It could be used to relay various analog and

digital information including television and radio broadcasts, telephone, telegraph, data transmission, and video transmission.

At 18:30 on 17 April, the Central Television Station conducted an approximately 1-hour test of television transmission; the picture was stable and sharp, the color was bright, and the audio channel was pure and clear. People in the Urumqi region, Kunming, and other areas were overjoyed to be able to watch a direct broadcast from the Central Television Station for the very first time.

3012/9599
CSO: 4008/97

NATIONAL DEVELOPMENTS

BRIEFS

GROUND STATION IN TESTING STAGE--The construction and installation project of the Urumqi meteorological satellite ground station, a priority project for the country, was checked and accepted by the government on the morning of 22 October. The project, which was prepared in 1978 and listed as a priority construction project for the country, involved an investment of some 11.86 million yuan and a construction area of some 7,640 square meters. After the completion of the construction and installation project, the ground station of the Urumqi meteorological satellite now enters the stage of testing equipment. It will be put into operation in the second half of next year. After starting operation, the ground station will undertake the task of receiving and processing meteorological information from (Fengyun) No. 1, a meteorological satellite to be launched by China next year, and transmitting the information to the Beijing meteorological center [Text] [Urumqi Xinjiang Regional Service in Mandarin 1300 GMT 22 Oct 86 HK]

/9716
CSO: 4008/12

PHYSICAL SCIENCES

FORECASTING METHODS FOR TURNING TYPE TYPHOONS IN EAST CHINA SEA

Beijing HAIYANG KEXUE [MARINE SCIENCES] in Chinese Vol 9, No 6, 9 Nov 85 pp 12-16

[Article by Fang Defeng [2075 1795 7685] of the Oceanography Institute of the Chinese Academy of Sciences, Beijing; Chinese Academy of Science Oceanography Institute Survey Research Report No 1233. This article benefited from the direction and encouragement of Professor Liu Fengshu whose assistance is especially acknowledged here.]

[Text] Turning type typhoons usually occur in the months of July, August, and September. These typhoons usually form in the northwest Pacific and move at a fixed speed toward the west and north. In the course of their motion the strength of the typhoons changes constantly. Coastal turning typhoons increase or stay the same in strength along our southeast coast but after landing these typhoons are weakened by the topography.

This article presents an analysis and forecast on typhoon surges at Dingdao and Wusong stations during turning typhoons in the East China Sea in recent years.

I. Characteristics of Turning Typhoons

A. Paths

1. Paths of turning typhoons at Wusong station: Apart from one or two, these typhoons basically can be classified under four types with differing paths (see Figure 1a). Path A represents turning typhoons which have hit land. Their point of landing is generally 119°-120° east and 24°-27° north (i.e., near Pingtan and Sansha) and their turning point usually does not exceed 118°-120° east and 31°-33° north. Path B represents typhoons which slightly scrape land as they turn. For them the landing is generally 119°-121° east and 25°-28° north (i.e., Pingtan and Sansha or slightly north) and they turn in a range of about 120°-122° east and 30°-32° north. Path C shows typhoons which turn at sea usually in a range of 122°-123.5° east and 31°-32° north. Path D crosses and turns beyond 126° east. Path BB shows typhoons landing and turning or lightly scraping the northern coast in the vicinity of Haimen and Shipu south of Hangzhou Bay and, just south of the mouth of the Yangtze, turning toward the Duima Strait.

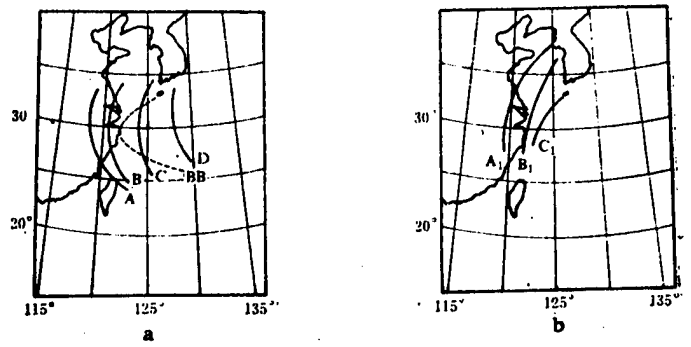

Figure 1. Schematic of Typhoon Path Types

2. Paths of turning typhoons at Qingdao station: these typhoons can be classified into three different paths (see Figure 1b). Path A_1 after landing and turning goes back out to sea from near Lianyun Harbor to the Korean Peninsula. Path B_1 after landing and turning goes back out to sea from south of Lianyun Harbor and north of Lüsi toward the Korean Peninsula. Path C_1 includes those that turn on land and those that turn at sea. The land turning type after turning heads out to sea from Lüsi or a little north and at sea goes toward the southern part of the Korean Peninsula. The sea turning type typhoons turn beyond the mouth of the Yangtze and go to the southern part of the Korean Peninsula or the Duima Strait.

B. Wind

Analysis and theoretical research on large quantities of observational data reveal that in the typhoon pass, wind is one of the major factors causing early continental shelf shallow-sea surges. According to a study of related research, wind speed and wind direction both have direct effects on surges.

1. Wind direction: for a particular observation station the wind direction is different, changing with the the typhoon's path, and the geographical conditions of the station also have an effect. Figures 2 and 3 show wind direction polar graphs of the paths of typhoons at the two stations of Qingdao and Wusong, respectively.

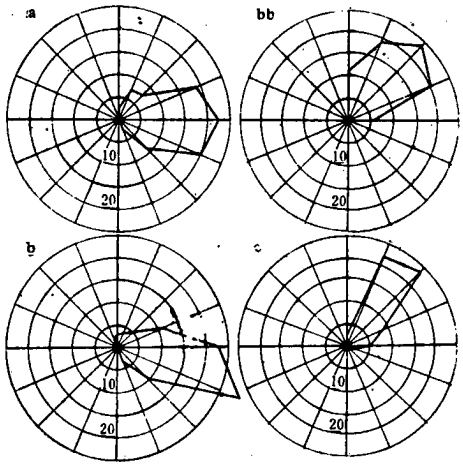

Figure 2. Wind Direction Polar Graphs for Wusong Station

a, b, c, and bb are wind directions for Wusong station Paths A (advanced 2 hours), B (advanced 4 hours, C (advanced 6 hours), and BB (correspondingly).

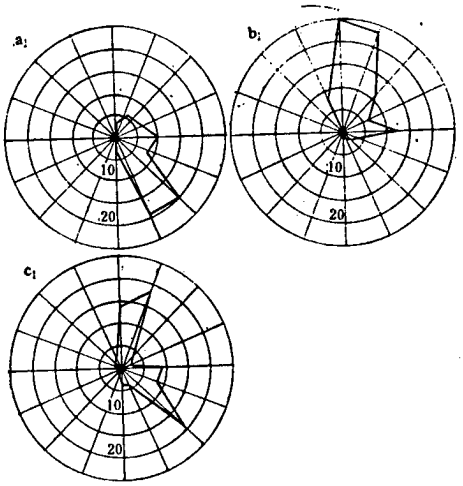

Figure 3. Wind Direction Polar Graphs for Qingdao Station

a, b, and c are wind directions corresponding to typhoon Paths A, B, and C, respectively.

2. Wind speed: according to wind speed data statistics for 18 turning type typhoon surges about 2-6 hours in advance at Wusong station, the relationship between typhoon surges and wind speed before the maximum surges is very close with correlation coefficients all 0.7 or above. Figure 4a shows a single wave following the typhoon described simply by using the wind (noted as Hw). The Qingdao station wind and surge have no obvious delay interval with the primarily northeast wind having the dominant effect on the advance surges.

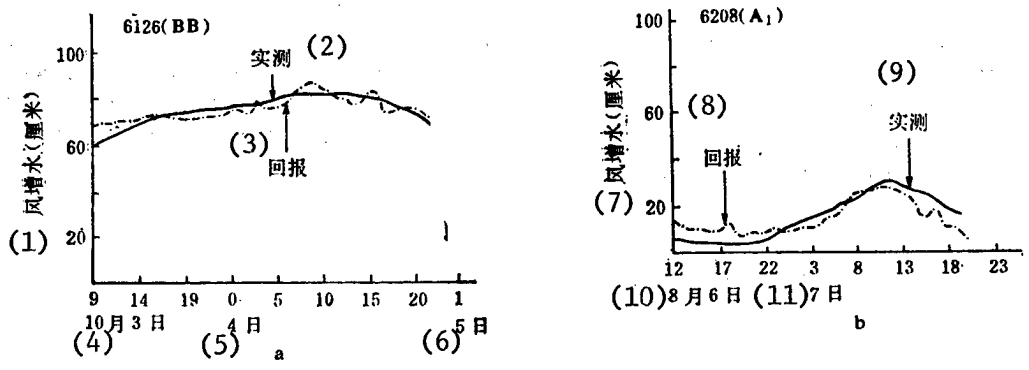

Figure 4. Wind Surge Recap Report Conditions

Key:

1. Wind Surge (cm)
2. Actual observations
3. Recap report
4. Oct 3 5. 4 6. 5
7. Wind Surge (cm)
8. Recap report
9. Actual observation
10. Aug 6 11. 7

C. Surges

Data analysis shows that the majority of turning typhoons which affect Wusong have surges appearing and that the sizes of the surges are different according to the typhoon's strength and path. Surge size is related to the strength of the typhoon. However, actual conditions are more complicated. As the typhoons follow different paths, the size of the surges produced and the forms of the surges are different.

The form of surges at the Wusong station are mostly of the "wave type" but each path has its own characteristics. The characteristic of Path C surges is that when the typhoon approaches the mouth of the Yangtze, the station is exactly in the region of maximum winds at the center of the typhoon and consequently causes severe surges. For example, in typhoon No 6207 the largest surges at Wusong were 220 cm. The form of surges for Path B is that when the typhoon is farther away from the station, the station just meets the effects of large on-shore winds and the water level begins slowly to rise. And when the typhoon reaches the station and turns, large off-shore winds appear and the water level falls, rapidly displaying an ebb phenomenon. For Path A, since the typhoon loses strength after landing, the typhoon surges also are much smaller than surges usually caused by typhoons along Path C.

The surges at Qingdao produced only by turning type typhoons generally seldom exceed 100 cm. Of these, Path A is before the typhoon arrives under the action of southeast winds, and the water level suddenly rises and later turning into northern winds, the water level falls rapidly and then connects with stronger oscillations. For Paths B_1 and C_1 the water level rises slowly.

II. Formulae for Forecasting of Turning Typhoon Winds

Analyzing several characteristics of turning type typhoon winds, based on the action of different path winds on surges we selected wind values from the surge process for instances of strong typhoon Nos 6208, 6126, 6615, 6207, and 5622 to be independent input values. In order to reduce mutual nonlinear effects we used a 13-hour filtering (see Figure 5) on the surge process and attempted to find a relationship between the remaining portion after filtering (denoted as ζH) and astronomical tidal forecast values. The results were still quite good for the front part of the surges.

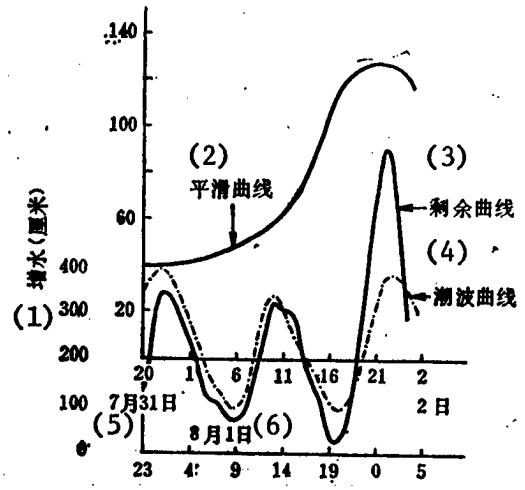

Key:
1. Surge (cm)
2. Smooth Curve
3. Residual
4. Tidal Wave
5. 31 July
6. 1 August

Figure 5. Smooth, Residual, and Tidal Wave Curves

1. Forecasting formulae: the ΔH part for Path C and Path BB at Wusong station preceded astronomical tide forecast values by 2 to 3 hours. The forecast formulae are composed of the superposition of the two parts above. The forecasting formulae are shown in Table 1 and Table 2.

Table 1. Wusong Station Forecasting Formulae

(1) 公式序号	(2) 预报公式	(3) 相关系数	(4) 剩余标准差 (cm)	(5) 显著性水平 (α)	(6) 绝对值百分比回报误差 (cm)	(7) 路径	(8) 备注
1	$Hw=4.17w+4.976$	0.90	7.074	0.01	76%(<16)	A	(9)Hw：风增水，单位cm；(10)w：提前2小时风值(m/s)；ΔH：天文潮引起的部分水位(cm)；(11)(12)ζ：天文潮预报值(cm)
	$\Delta H=0.127\zeta-31.341$	0.74	6.437	0.01	80%(<19)		
2	$Hw=1.21w+15.974$	0.72	2.611	0.01	91%(<12)	B	w：提前4小时的风值，其(13)它符号同上
	$\Delta H=0.104\zeta-23.464$	0.78	5.813	0.01			
8	$Hw=15.111w-35.085$	0.88	17.224	0.01	75%(<23)	C	(14)w：提前6小时风值；ζ：迟后2小时的天文潮预(15)报值，其它符号同上
	$\Delta H=0.209\zeta-52.582$	0.94	7.590	0.01			
4	$Hw=2.034w+57.544$	0.78	3.595	0.01	91%(<13)	BB	(16)w：对应的风值；ζ：迟后3小时的天文潮预(17)报值，其它符号同上
	$\Delta H=0.146\zeta-30.699$	0.70	6.437	0.01			

Key:

1. Formula No
2. Forecasting formula
3. Correlation coefficient
4. Residual standard deviation
5. Significance level
6. Absolute value percentage delay report error
7. Path
8. Notes
9. Wind surge (cm)
10. Wind value 2-hour advance (m/s)
11. Part of water level caused by astronomical tides (cm)
12. Astronomical tide forecast value (cm)
13. Wind value, 4-hour advance
14. Wind value, 6-hour advance
15. 2-hour delay astronomical tide forecast value
16. Corresponding wind value
17. 3-hour delay astronomical tide forecast value

Table 2. Qingdao Station Forecasting Formulae

(1) 公式序号	(2) 预报公式	(3) 相关系数	(4) 剩余标准差 (cm)	(5) 显著性水平 (α)	(6) 绝对值百分比回报误差 (cm)	(7) 路径	(8) 备注
5	$Hw=1.657w-1.302$ $\Delta H=0.036\zeta-10.204$	0.80 0.61	5.580 6.504	0.01 0.01	79%(<17)	A_1	(9) Hw：风增水，单位cm； (10) w：对应风值(m/s)； ΔH：天文潮引起的部分水位 (cm)； (11) ζ：天文潮预报值 (cm) (12)
6	$Hw=1.441w+14.614$ $\Delta H=0.039\zeta-13.440$	0.82 0.78	4.463 4.486	0.01 0.01	96%(<14)	B_1	(13) 符号同上
7	$Hw=0.720w+24.950$ $\Delta H=0.085\zeta-19.224$	0.74 0.85	2.341 3.507	0.01 0.01	91%(<13)	C_1	(14) 符号同上

Key:

1. Formula No
2. Forecasting formula
3. Correlation coefficient
4. Residual standard deviation
5. Significance level
6. Absolute value percentage delay report error
7. Path
8. Notes
9. Wind surge (cm)
10. Corresponding wind value (m/s)
11. Part of water level caused by Astronomical tides (cm)
12. Astronomical tide forecast value (cm)
13. Same
14. Same

2. Selection of forecast intervals: apart from wind direction which are based on previous discussions, we must consider the paths.

For Wusong station Path A, the forecast beginning point generally was when the typhoon reached the vicinity of 120° east and 24°-25° north, "aged" 20-30 hours. For Path B the forecast beginning point was generally when the typhoon reached the vicinity of 121° east and 25° north, and the largest surges took place before the typhoon reached the station, forecasting ahead 20-30 hours. For Path C the forecast beginning point was when the typhoon reached the area of 126° east and 25° north, forecasting ahead 20-30 hours. And for Path BB the forecast beginning point was when the typhoon reached around 125° east and 25° north, forecasting ahead 20-30 hours. When the typhoon had left the affected region just a little, the station experienced strong off-shore winds and surges quickly subsided or reduced waters appeared. These are the problems which a forecasting interval must strictly master.

For the Qingdao station Path A_1, the forecast beginning point is when the typhoon reaches the area 119° east and 28° north. The maximum surges occurred before the typhoon arrived, forecasting 20-35 hours. For Path B_1, the forecast beginning point was generally when the typhoon reached the neighborhood

of 121° east, 29°-30° north, forecasting 20-35 hours. Path C_1's forecast beginning point was when the typhoon reached 123° east, 29°-31° north, forecasting 20-35 hours. The selection of the Qingdao station interval ought to draw our interest since it begins surges when the typhoon has not yet "put to sea." The time of on-shore winds of the typhoon as it puts to sea is very short because it quickly leaves. It is precisely at this time that the off-shore winds are great and the water level quickly drops.

III. Delay Reports and Test Reports

Based on the forecasting equations established for different paths their conditions of fit can use the formulae described above to do delay report computations on the entire input sample.

Figures 6a and 6b give the delay report conditions of the surge process for representative typhoons at the two stations of Wusong and Qingdao. Of these, Paths A_1, B_1, and C_1 for Qingdao station and Paths A and B for Wusong station have an optimal advance of 3 hours (for example, the 8 o'clock surge in the delay report is actually a 5 o'clock surge). This is roughly because of the time delay created by filtering.

Paths C and BB at Wusong station have no 3-hour advance, possibly because the ΔH portion has an obvious 3-hour advance which just makes up for the time delay due to filtering.

Figures 7a and 7b give the test report conditions for representative typhoon surge processes at Wusong and Qingdao. Of these, Paths A, B, A_1, B_1, and C_1 still are advanced 3 hours at best (the reason is the same as for the delay reports).

From the conditions of fit for recap report and test report surge processes above, whenever the surge conditions are such that the maximum surge strength and the fluctuation are larger the peak value location appears low in the forecast. The relationship between these phenomena and a single wave traveling with the typhoon is not great and is mostly created by the ΔH part after filtering. At the time the typhoon surge is large, the ΔH part is also large, and the larger the surge the larger this part gets. But the tidal forecast portion has no change (see Figure 5); consequently a larger disparity appears.

In order to resolve the problem of maximum peak value location, from an analysis of a large quantity of data we obtain a 2-3 hour correction before or after the maximum value location (see Table 3).

Table 3. Maximum Value Location 2-3 Hour Correction

(1) 增 水 (厘米)	(2) 校正 (厘米)
>70—80	+10
>100	+20
>140—150	+40

Key:
1. Surge (cm)
2. Correction (cm)

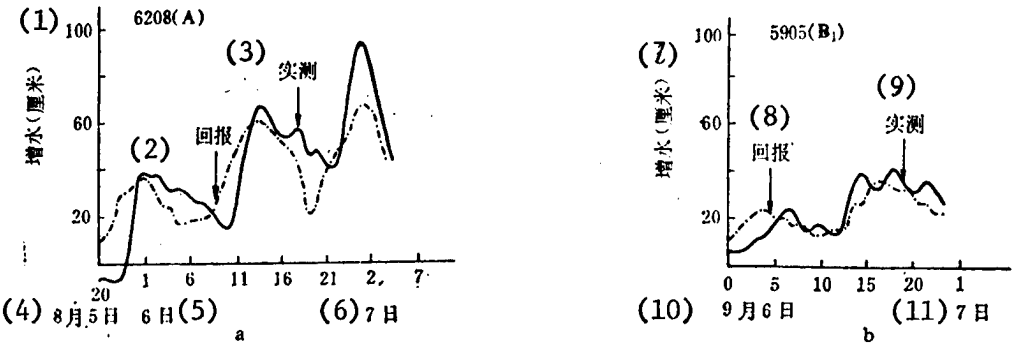

Figure 6. Surge Recap Report Conditions

a. Wusong typhoon No 6208 surge recap conditions formula (1)
b. Qingdao typhoon No 5905 surge recap conditions formula (6)

Key:

1. Surge (cm)
2. Recap
3. Actual observation
4. 5 August
5. 6
6. 7
7. Surge (cm)
8. Recap
9. Actual
10. 6 September
11. 7

For some maximum peak value locations lower than 70 cm the errors are all within a standard deviation. If the strength or fluctuation of the surge is larger the peak value location can take into consideration a 5-10 cm addition.

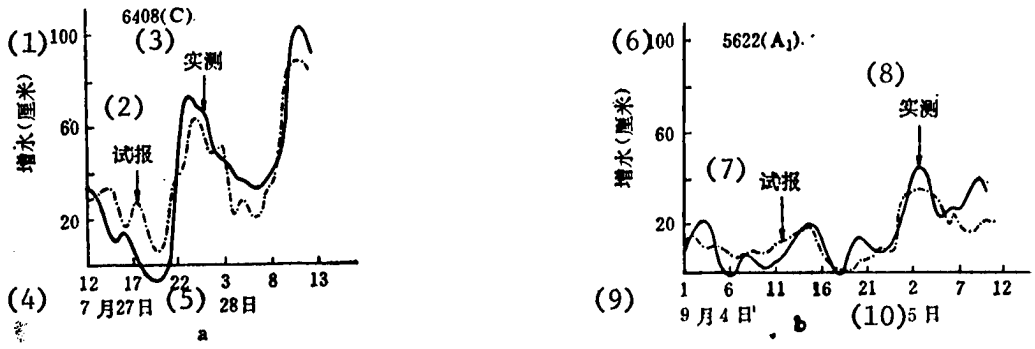

Figure 7. Test Report Conditions at Wusong and Qingdao

a. Wusong typhoon No 4608 surge test report formula (3)
b. Qingdao typhoon No 5622 surge test report formula (5)

Key:

1. Surge (cm)
2. Test
3. Actual
4. 27 July
5. 28
6. Surge (cm)
7. Test
8. Actual
9. 4 September
10. 5

IV. Conclusion

1. For previous turning type typhoons the storm sea level at Wusong station was higher and of these the levels produced by Path C type turning typhoons were the highest, reaching 5.75 meters. This is because the strength of marine typhoons is great and the range large. Their motion is slow and the period over which they continue is long and easily overcomes astronomical tide factors. Next comes Path BB whose surges are second only to those caused by typhoons which traverse Path C. The surges caused by typhoons on the other paths are less than this by half or more. At Qingdao station the surges produced by Path C_1 are larger, reaching 80 cm or more. The surges produced by other turning type typhoons are relatively smaller.

Experiments show that for single-station forecasting and a fixed path, faster forecasting can be done relying only on winds and tides at the place and that this is practical from the point of view of disaster precautions. But it must be specially noted that the surges simulated by the above formulae have reference only to the station itself. We cannot use the formulae for Station A to simulate the surges at Station B. Local winds and tides are affected by local geography and hydrological conditions and can only apply to the said locale.

2. The nonlinear problem. From relevant documents we see that in shallow-water harbors the nonlinear effects are very complicated. The analytical results of this paper show that the significance is less of nonlinear mutual effects at Qingdao station during the surge pre-period. When typhoons traverse Paths C and BB at Wusong station, the surge process nonlinearity mutual effects are very prominent. For Paths A and B during the surge post-period these sorts of mutual effects are also rather noticeable.

The forecasting formulae for different paths given by this paper, in terms of accuracy, are no lower than many previously adopted experiential and statistical forecasting methods and the forecast periods are also more satisfactory. If one wanted to extend the period one should note that the wind factors are not sufficient. We must have air pressure, speed, wind zones, and wind times as well as changes of the path on a small scale, all of which require further study. In addition, the degree of accuracy of the forecasting time zones selected depends on the accuracy of the meteorological section with regard to the typhoon path forecasting. As typhoon path forecasting develops, the precision of typhoon surge forecasting will also increase.

12966/12859
CSO: 4008/1002

PHYSICAL SCIENCES

FUZZY CLUSTER ANALYSIS OF POLLUTED SEABOARD ZONES

Beijing HAIYANG KEXUE [MARINE SCIENCES] in Chinese Vol 9, No 6, 9 Nov 85 pp 36-38

[Article by Yang Tailong [2799 1837 7127] of the Nanhai Fisheries Institute, Fisheries Academy of China]

[Text] Since the seventies, internationally known fuzzy cluster classification analysis methods have been frequently used to resolve soil classification problems. Recently fuzzy cluster analysis has been broadly applied to meteorology, geology, agriculture, forestry, and medicine.

This article applies fuzzy cluster analysis to carry out a cluster analysis with respect to the "composite data of actual values of observed water pollution of the Pearl River estuary seaboard." It provides pollution zones to improve environmental protection and lays a scientific basis for developing the fishery industry. There are many types of fuzzy cluster analyses. This paper adopts that compiled by Ding Shisheng.

I. Water Pollution Fuzzy Cluster Analysis

A. Water Pollution Fuzzy Clusters

1. Sample and cluster factor selection: this paper is based on the 9 types of water pollutants measured at 15 observation stations in the Pearl River estuary seaboard in March 1981 [1], (see Table 1).

2. Seeking a correlation: we used the following formulae on the water pollution indexed data to carry out standardization processing to facilitate obtaining the correlation relationship

$$X'_{ij} = \frac{X_{ij} - \overline{X}_i}{s_i}$$

in which

$$\overline{X}_i = \frac{1}{5} \sum_{j=1}^{15} X_{ij}, \quad s_i = \sqrt{\frac{\sum_{j=1}^{15} (X_{ij} - \overline{X}_i)^2}{15 - 1}}$$

X'ij represents the standardized data, $\overline{X}_i$ is the average value of the ith factor over the 15 stations, and S_i is the standard deviation of the ith factor.

Table 1. Actual Values of Various Observed Factors (x) (mg/L)

(1) 因子 x / 测站 (2)	COD	ΣHg	Cu	Pb	Zn	Cd	(4) 油类	(5) 有机氯农药	(6) 酚
01	3.10	0.000055	0.006	0.012	0.064	0.0006	0.144	0.002005	0.0039
04	1.12	0.000029	0.004	0.011	0.064	0.0011	0.068	0.000829	0.0080
46	1.68	0.000030	0.004	—	0.042	0.0020	0.059	0.002120	0.0117
07	0.60	0.000051	0.004	0.011	0.075	0.0015	0.084	0.001430	0.0061
08	0.43	0.000024	0.004	0.011	0.073	0.0006	0.104	0.001480	0.0040
10	0.27	0.000007	0.005	0.007	0.076	0.0012	0.105	0.001906	0.0084
12	0.21	0.000017	0.006	0.006	0.088	0.0017	0.091	0.001508	0.0040
14	0.34	0.000029	0.006	0.010	0.053	0.0026	0.116	0.001190	0.0070
16	0.34	0.000021	0.004	0.008	0.068	0.0024	0.131	0.000732	0.0024
19	0.96	0.000018	0.005	0.006	0.034	0.0012	0.084	0.001120	0.0076
20	1.16	0.000024	0.008	0.010	0.046	0.0006	0.100	0.001610	0.0078
23	0.79	0.000004	0.004	0.004	0.034	0.0004	0.068	0.001124	0.0037
26	0.48	0.000027	0.004	0.012	0.083	0.0013	0.082	0.001202	0.0027
30	0.54	0.000033	0.005	0.014	0.090	0.0016	0.090	0.000812	0.0099
32	0.61	0.000024	0.005	0.012	0.020	0.0024	0.094	0.000792	0.0051
(3) $\overline{Ci}$(平均)	0.84	0.000026	0.005	0.010	0.061	0.0014	0.095	0.001324	0.0062

Key:

1. Factor
2. Station
3. Average
4. Petroleum
5. Organic Chlorine Pesticides
6. Phenol

3. Betting the fuzzy correlation matrix: using the standardized data (table omitted) we compute the fuzzy correlation coefficient:

$$\gamma'_{ij} = \frac{\sum_{k=1}^{9} X_{ik} X_{jk}}{\sum_{k=1}^{9} X^2_{ik} \sum_{k=1}^{9} X^2_{jk}}$$

$$(i, j = 1,2,\cdots, 15)$$

The correlation matrix R' is given below:

1.0000	0.9994	0.9999	0.9919	0.9743	0.9233	0.8763	0.9548	0.9364	0.9992	0.9992	0.9991	0.9833	0.9984	0.9989
0.9994	1.0000	0.9993	0.9954	0.9800	0.9334	0.8908	0.9606	0.9439	0.9993	0.9994	0.9995	0.9886	0.9967	0.9973
0.9999	0.9993	1.0000	0.9912	0.9725	0.9205	0.8737	0.9518	0.9330	0.9987	0.9987	0.9986	0.9823	0.9987	0.9993
0.9919	0.9954	0.9912	1.0000	0.9943	0.9632	0.9301	0.9804	0.9695	0.9953	0.9956	0.9960	0.9983	0.9847	0.9857
0.9743	0.9800	0.9725	0.9943	1.0000	0.9859	0.9605	0.9949	0.9899	0.9819	0.9821	0.9827	0.9974	0.9618	0.9631
0.9233	0.9334	0.9205	0.9632	0.9859	1.0000	0.9910	0.9918	0.9968	0.9370	0.9373	0.9384	0.9747	0.9028	0.9051
0.8763	0.8908	0.8737	0.9301	0.9605	0.9910	1.0000	0.9662	0.9785	0.8921	0.8929	0.8946	0.9486	0.8523	0.8551
0.9548	0.9606	0.9518	0.9804	0.9949	0.9918	0.9662	1.0000	0.9980	0.9659	0.9659	0.9664	0.9852	0.9384	0.9400
0.9364	0.9439	0.9330	0.9695	0.9899	0.9968	0.9785	0.9980	1.0000	0.9494	0.9494	0.9502	0.9777	0.9171	0.9190
0.9992	0.9993	0.9987	0.9953	0.9819	0.9370	0.8921	0.9659	0.9494	1.0000	1.0000	1.0000	0.9882	0.9956	0.9962
0.9992	0.9994	0.9987	0.9956	0.9821	0.9373	0.8929	0.9659	0.9494	1.0000	1.0000	1.0000	0.9887	0.9956	0.9963
0.9991	0.9995	0.9986	0.9960	0.9827	0.9384	0.8946	0.9664	0.9502	1.0000	1.0000	1.0000	0.9893	0.9954	0.9961
0.9833	0.9886	0.9823	0.9983	0.9974	0.9747	0.9486	0.9852	0.9777	0.9882	0.9887	0.9893	1.0000	0.9740	0.9750
0.9984	0.9967	0.9987	0.9847	0.9618	0.9028	0.8523	0.9384	0.9171	0.9956	0.9956	0.9954	0.9740	1.0000	0.9997
0.9989	0.9973	0.9993	0.9857	0.9631	0.9051	0.8551	0.9400	0.9190	0.9962	0.9963	0.9961	0.9750	0.9997	1.0000

4. Getting the fuzzy matrix: $\gamma_{i,j} = 0.50 + \gamma'_{i,j}/2,$

Fuzzy matrix:

$$R = \begin{pmatrix} 1 & r_{1,2} & r & \cdots & r_{1,15} \\ r_{2,1} & 1 & r_{2,3} & \cdots & r_{2,15} \\ r_{3,1} & r_{3,2} & 1 & \cdots & r_{3,15} \\ \vdots & \vdots & \vdots & & \vdots \\ r_{15,1} & r_{15,2} & r_{15,3} & \cdots & 1 \end{pmatrix}$$

5. Getting the fuzzy equivalent matrix: fuzzy matrices do not all necessarily possess "transferability." To get its fuzzy equivalent matrix this paper computes the transferability satisfied "when R^4 is reached." Thus R^4 is its "transfer closure" and the matrix it forms is the fuzzy equivalence relationship matrix denoted as R*.

6. Cluster results: The λ---- section set of the fuzzy equivalence relationship matrix is a common equivalence relationship R_λ. Based on these equivalence relationships, the elements in R* can be clustered at any level of confidence λ and form a dynamic cluster figure (Figure 1).

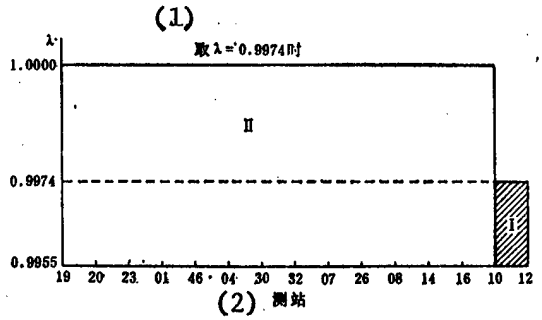

Key:
1. With
2. Station

Figure 1. Water Pollutants Cluster

Carrying out classification on Pearl River estuary seaboard pollution, all the stations are divided into two kinds. Apart from the water of station No 12 which belongs to type I, the water of the remaining 14 stations belongs to type II (see Figure 2).

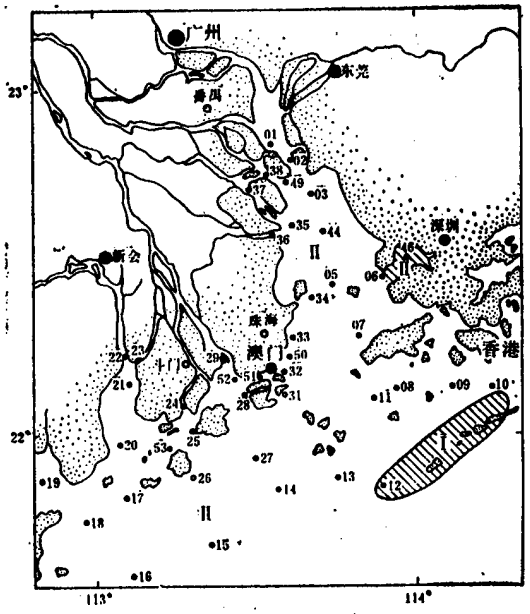

Figure 2. Water Quality Zones

B. Analysis of Cluster Results

From the cluster results we know the water of station No 12 belongs to type I and the rest belongs to type II. From the actual measured values of the water we see that the value of COD at station No 12 is the smallest of all the measuring stations and that the measured Pb and phenol are less. According to the marine water quality standards of Figure 2, that the water of station No 12 belongs to type I is in line with reality. From Table 1 we see that the Hg of station No 10 is the smallest of all the stations and that COD and Pb are also smaller. At station No 16, Cu and phenol are the smallest. Therefore the water of stations No 10 and 16 also could belong to type I but from the point of view of surveying the marine region we tend to group them as type II and all the other stations belong to type II as well (see Figure 2).

II. Conclusion

The marine pollution demarcations completed by the application of fuzzy cluster analysis with respect to dividing into types and positioning within the classification system need not be classified by people, thus avoiding subjectivity.

From the history of marine pollution we see that the disparities of a regional nature are very great. Even in the same region the marine pollution conditions are not entirely the same and there are also cases of divisions of severity. Consequently, an intensified study of the patterns of Pearl River estuary marine pollution is extremely significant for more effective Pearl River environmental protection and for the expansion of fishery production.

Table 2. Marine Pollution Evaluation Standard (S) for each Important Factor [1]

S (1)因子 / (2)类别		ΣHg	Cu	Pb	Zn	Cd	COD	(4)油类	(5)有机氯农药	(6)挥发酚
(3)海水	Ⅰ	0.0005	0.01	0.05	0.1	0.005	<3	0.05	0.001	0.005
	Ⅱ	0.001	0.1	0.1	1	0.01	<4	0.1	0.02	0.01
	Ⅲ	0.001	0.1	0.1	1	0.01	<5	0.5	0.04	0.05

Marine items cited from the national marine water quality standards (mg/L).

Key:

1. Type
2. Marine
3. Factor
4. Petroleum
5. Organic Chlorine Pesticides
6. Volitile phenols

2966/12859
CSO: 4008/1002

PHYSICAL SCIENCES

LSIS-II LAYOUT SYSTEM DESCRIBED

Beijing BANDAOTI XUEBAO [CHINESE JOURNAL OF SEMICONDUCTORS] in Chinese Vol 7 No 3, May 86 pp 284-291

[Article by Bao Chunhua [7559 2504 5478] and Zhuang Wenjun [8369 2429 0689] of the Chinese Academy of Sciences Institute of Semiconductors]

[Text] This article introduces a subsystem developed by our institute for verification of the correctness of contact connection in a LSIS-II layout design system. This subsystem's heuristic verification system takes 10 verification principles as the basis of its algorithm, adopts hierarchical checking methods and, in order to increase the error hit rate, uses directional and regional auto-locking techniques. The subsystem gets satisfactory results and establishes a reliable foundation for designs utilizing LSIS-II systems to carry out LSI/VLSI design.

I. Introduction

The description of contact connections between cells (including pseudo-cells) is an important constituent part of layout design with regard to abstract description and of whether or not the correctness of the contact connections will directly influence design mass and design efficiency. In various processes from circuit design and description to input, there only needs to be unavoidable artificial interference and sundry random errors occurring. If they do not undergo some means to discover the errors in them the situation will lead to a whole set of connection errors in subsequent layout design and in masking processes so that in the end rejects are produced which in larger circuits will entail great loss. Consequently, contact connection correctness verification is something that cannot be slighted. Discovery of errors and their elimination is the foundation and premise for carrying out the design of subsequent parts of the entire system.

The present verification subsystem, based on basic principles of circuit design and on human design experience, is summed up in 10 verification principles with regard to performing inspection for errors in contact connection. The theory and practice are both completely explained and this heuristic verification subsystem has very high efficacy with a rate of error recovery going above 95 percent. The subsystem can uncover random errors which come about in the various stages of human interference including entry

error, description error, and errors in partial designs (logical errors or electronic errors). It also has very good functions for location of uncovered errors. The error information can be directly viewed in great detail for the ease of user correction. Because the algorithm adopts hierarchical checking as well as directional and positional auto-locking techniques, pseudo-error and derived error information is greatly reduced, effectively increasing the error hit rate and consequently the correction efficacy as well as making the subsystem have a modularized structure and greater flexibility.

II. Algorithm Basis of the Verification Subsystem

1. Establishment of Verification Principles and Analysis of the Error Recovery Rate

Since a verification system ought to inspect exhaustively for errors in the verification objective, even if the error recovery rate approaches or reaches 100 percent, the level of the error recovery rate is determined by the means used to verify as well as whether or not the method used is complete.

Adopting heuristic principles we structured a heuristic verification system. Based on basic principles of circuit design and human design experience the system comes down to 10 verification principles. Each time one of these principles is violated there is an error. Below we discuss the establishment of these verification principles and the error recovery rate.

A. Conditions for the Completeness of the Established Verification Principles

Let the already established verification principles be A_1, A_2, ..., A_{n-1}, and a new verification principle be A_n. Let the set of errors which can be uncovered by A_1, A_2, ..., A_{n-1}, A_n be M_1, M_2, ..., M_n. Then we ought to have:

i) $M_n \neq \phi$.

ii) M_n is not a subset of $\bigcup_{i=1}^{n-1} M_i$.

We use the set graph to the right to indicate the situation for verification principle error recovery. Let the set of errors which can occur be E.

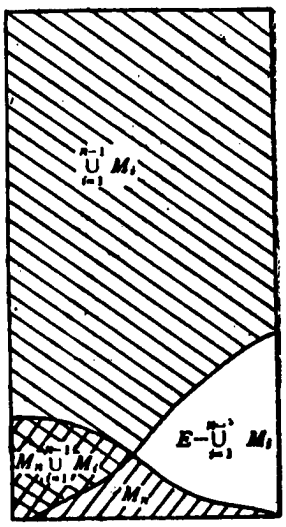

Figure 1. Schematic of Verification Principle Effectiveness.

The level of a verification principle's usefulness can be considered from the three conditions below. The more conditions met the higher the efficacy.

i) M_n as large as possible.

ii) $M_n \cap \bigcup_{i=1}^{n-1} M_i$ as small as possible.

iii) Degree of positionality as high as possible.

So for a group of verification rules, A_1, A_2, ..., A_k, the level of efficacy can be examined from the following points. The more conditions met the higher the efficacy.

i) $\bigcup_{i=1}^{k} M_i$ as large as possible.

ii) For any $1 \leq i \leq K$, $M_i \cap (\bigcup_{j=1}^{k} M_j)$ as small as possible.

iii) The number of principles contained, K, as small as possible.

iv) Degree of positionality as high as possible.

The 10 verification principles of our verification subsystem are as follows:

i) Existence of the cell.

ii) Existence of the terminal point.

iii) Nonuniqueness of the cell.

iv) Independence of the circuit network.

v) Existence and uniqueness of special terminal points.

vi) Necessary bridging of special terminal points.

vii) Correspondence of terminal points with circuit networks.

viii) Reasonableness of cell selection.

ix) Conventional principles.

x) Syntactic rules

B. Analysis of the Error Recovery Rate

Investigation of the error recovery rate necessitates making a comparison of all possible errors which can occur with the errors which the verification rules are capable of detecting. We take an analysis of errors with respect to a circuit network surface as an example.

If we analyze the errors which can occur for a circuit network surface we see that they can be divided into a few categories such as:

i) Syntax errors.

ii) Element code (cell code or terminal point code) errors.

Here we can also make a division between wrong and mistaken notation:

Wrong notation: 100-201 incorrectly written as 1000-201 when a 1000 code cell does not exist.

Mistaken notation: 20-201 mistakenly written as 21-201 when a 21 code cell does exist.

iii) Leakage point (in special situations a leakage network).

iv) Multiple point (in special situations a multiple network).

v) Continuity errors in the design apart from the errors noted above.

The random errors which occur in circuit network surfaces in the vast majority of cases, are subordinate to the error categories described above and each error category generally correspondingly can be uncovered by a union of some verification rules.

For example, an element code error can be uncovered by the union of rules for existence of the cell, existence of the terminal point, independence of the circuit network, and the existence and uniqueness of special terminal points. Wrong notation of an element code can be detected by existence of the cell and existence of the terminal point; mistaken notation of an element code can be found by independence of the network and existence and uniqueness of special terminal points.

As above, it can be seen from the analysis of various errors and the efficacy of the verification principles that the verification rules of our subsystem have a high error recovery rate.

Outside the area of errors which can be uncovered by the 10 verification rules there are two kinds of situations that exist. In one kind there are some odd types of errors that cannot be uncovered in theory working from design principles and experiential rules. For example, in two mutually independent circuit networks two points with the same electronic properties are interchanged. This sort of error under general conditions could not be uncovered by verification rules. But in actuality the probability of occurrence of this sort of error is extremely small. Experimental results also prove this point. In the other kind of situation there are odd types of errors where from design principles and experimental rules the verification results have an indeterminateness. These have a direct relationship to special features of human design views and concrete objectives and in the end require humans to make definitive verification.

In order to increase the error recovery rate dealing with the second situation, in addition to the 10 principles, we also designed some critical principles for possible mistakes in critical states to give a warning message to alert people to inspect and determine whether or not the situation is correct. Consequently errors which are present are discovered raising the

error recovery rate. Figure 2 indicates the error recovery situation after the application of critical principles.

Figure 2. Schematic of Critical Principles Raising the Error Recovery Rate

2. Error Position

In a verification system people want not only to be able to uncover the presence of errors. They also desire to know the precise location of the error to aid in correction reducing user frustration and increasing usefulness.

Because the verification principles themselves possess high positional capabilities, the verification results of our subsystem are able to give error locations with a rather high precision. In an actual verification case which had 52 random errors the error information output had 69.2 percent located at a nodal point, 25 percent at two nodal points, and 5.8 percent at a circuit network (for a recovery rate of 100 percent).

3. Hierarchical Checking

Because the LSIS-II system adopts hierarchical descriptions for describing circuits we adopted methods of hierarchical checking in the verification subsystem to deal with this special feature.

Hierarchical checking is just making an ordering according to the nesting relationships between the pseudo-cell and performing checks level by level beginning from the lowest pseudo-cell (Adopting the cell concept in hierarchical design, the entire board can be treated as the largest, the highest level pseudo-cell). Hierarchical checking raises the effective rate of error detection and avoids many complicated inspections. Also design objectives which use hierarchical descriptive syntax have greater flexibility during inspection and at the same time make the subsystem structure completely clear forming a modular structure.

4. Methods for Increasing the Rate of Error Hits

In general verification systems, in order to facilitate revision, usually there is concern not only for the error recovery rate but also a desire to have a higher error hit rate, that is reduce as much as possible extraneous error information--the appearance of derived errors and pseudo-error information.

Because the verification rules of our subsystem are by no means mutually independent, there exist intersections between the errors uncovered by each rule. This is shown in Figure 3. Sometimes, a single error can be detected by several principles individually but there are differences in the degree of positionality.

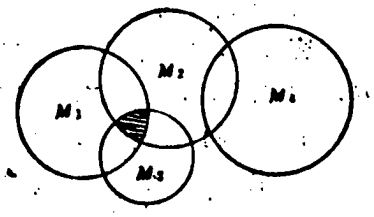

Figure 3. Schematic of the Non-Independence of Verification Principles

For example, 21-101 is an input terminal point and it has been incorrectly written as 121-101 and a 121 code cell does not exist. This error can be detected by the three principles of: 1) existence of the cell, 2) existence and uniqueness of special terminal points, and 3) necessary bridging of special terminal points. If these three rules are used in sequence in one inspection pass then three lines of error information will be put out corresponding to this one error of which two lines are derived error information. When this error has been corrected the three lines of error information can be deleted with it.

With two different level pseudo-cells, the appearance of an error in the lower level pseudo-cell can effect certain verifications in the higher level pseudo-cell. On these occasions there is a chance of producing pseudo-error information. Separately, if an important part in the input information produces an error, it can lead to connection errors in various parts accompanied by large amounts of pseudo-error information. Sometimes a single error produces as much as several times to dozens of times as much pseudo-error information. An example of this is when in a cell code type code correspondence table omits a cell code. Then terminal points connected with this cell in circuit networks bring about great quantities of pseudo-errors because the cell code is considered not to exist.

In order to reduce derived error and pseudo-error information and raise the rate of error hits, we engaged in analysis of the linkage relationship between various types of error information corresponding with the verification principles. Adopting techniques of positional autolocking and regional autolocking made the error hit rate improve.

Positional autolocking is based on the relationship between various verification principles. After using a certain principle to discover an error, controls are applied over whether or not to carry out particular verification principles which have a derivative relation to that principle or over whether or not to carry out inspection in a particular scope consequently

avoiding the production of derived error information. We call this "applied locking."

Regional autolocking is based on the linkage relationship between errors of various described regions. When a certain kind of error is discovered in a certain region, control is applied over whether or not to carry out an inspection of described regions which are severely effected by this region's errors, also thereby avoiding the production of pseudo-error information.

Adoption of positional autolocking and regional autolocking techniques reduces the repeated unnecessary inspection of the same error. It also reduces superfluous derived errors and pseudo-error information. This raises the efficacy of revisions. But another aspect is that because "locking" has been introduced there is the possibility of locking out real errors but after the error indicated by the error information on the previous pass is truly corrected, during the next inspection the lock corresponding to the error which has been corrected is opened and the real error locked out by this lock will be freed and so it can be guaranteed that the autolocking method does not lower the error recovery method. The difference is that errors are detected in batches and corrected in batches. After the one batch is corrected the next batch is detected on the subsequent pass and the process repeated until no error information is output. This makes each batch of error information have a very high hit rate, greatly reducing the user's work to discern whether or not the error is real, facilitating revision.

We use Figure 4 below to represent symbolically the autolocking relationship between errors after application of autolocking techniques.

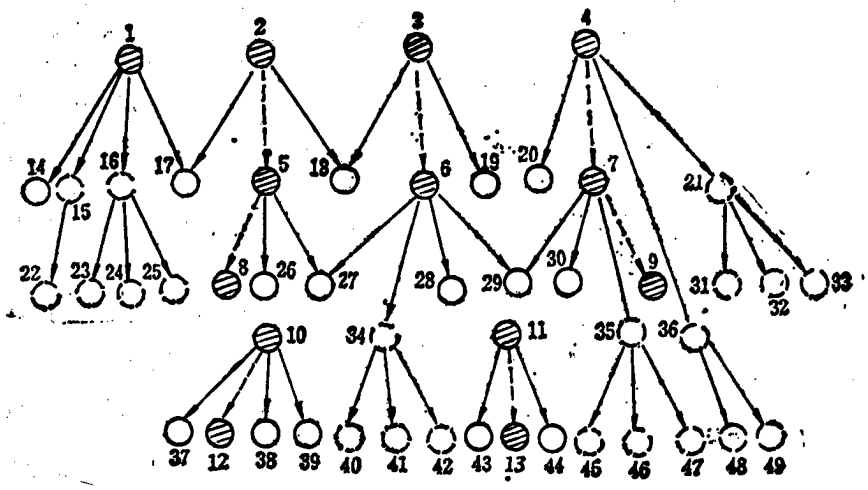

Figure 4. Error Autolocking Tree

● stands for real errors

○ stands for derived errors

◌ stands for pseudo-errors

In the figure a directed line between points A and B indicates there is an autolocking relationship between A and B. That is, only after error A has been discovered and eliminated can error B be detected.

i) A solid directed line from A to B is denoted as W_t, A $\rightarrow$ B and means:

Objectively, B is derived error information from A. After error A has been detected and eliminated, only then can B be inspected. (At this time, error B could disappear due to the elimination of error A.)

ii) A broken directed line from A to B is denoted W_t, A $\dashrightarrow$ B and means:

Objectively, B is not derived error information from A but because of the effect of "locking" introduced during inspection an "autolocking" was also produced between A and B. That is, after error A has been found and eliminated, only then can error B be inspected and discovered.

From the figure we can see that if autolocking techniques were not used although it would only have required the correction of ⊘ circle numbered errors (13 in the figure) to eliminate all the error information yet the error information of all the numbered circles could be output (49 in the figure) and the user based on 49 items of error information in the end would only need to fix 13 thus obviously increasing the amount of work to discern which were the real errors. However, with the introduction of "locking" the O and ◌ information, the derived errors and pseudo-error information, is vastly reduced giving the user a very significant convenience.

Use of error autolocking techniques increases the rate of error hits but under general conditions can also increase the number of runs. The number of runs and the error hit rate are in contradiction to each other. If we raise the error hit rate then the number of runs is increased and if we reduce the number of runs it can lower the error hit rate. Therefore, how to look after both aspects at the same time is a very important question which directly relates to the processing efficiency of the subsystem. Resolution of this problem is closely related to how to "apply locking" for inspection.

Below we discuss the problem of how to apply locking. Define the maximum chain length as L_{max}.

Let the various apex with entry degree 0 in the error autolocking figure be $V_{i1}, V_{i2}, \ldots, V_{in}$ and those with exit degree 0 be $V_{j1}, V_{j2}, \ldots, V_{jm}$. Let the line weight of the various directed lines be 1 and let the path from any V_{iR} to V_{jP} be L_{kp}, then

$$L_{max} = \max_{\substack{k=i_1,\ldots,i_n \\ p=j_1,\ldots,j_m}} \{L_{kp}\}.$$

Thus if we let the number of runs be q (i.e. after the qth run there is no error information output) then

$$q = L_{max} + 2.$$

Now how do we apply locking so as to ensure higher processing efficiency? After applying locking we should have:

i) L_{max} as small as possible,

but also have

ii) The apex intervals, W_t as few as possible. (The error information output for each run is an apex in the figure.)

In actual problems the concrete calculation of the length of L_{max} is in practice very difficult. Consequently during actual processing taking i) and ii) above for guidance we adopt the method of carrying out point by point analysis of the various verification principles and the nature and relationship of the errors to determine how to apply locking. We consider the following factors:

i) The probability of error occurrence corresponding to each principle,

ii) The probability of derived errors and pseudo errors led to by each type of error,

iii) The ratio of probabilities of the number of derived errors locked out by the application of locking with respect to a certain principle to the number of real errors. If the individual number of W_t (quantity of linkage errors) is far greater than the individual number of W_p (quantity of real errors locked out) then we consider applying locking, otherwise it is not considered and so on.

As above, because in our subsystem we engaged in comprehensive analytical considerations, adopting means with better goodness of fit to deal with both aspects, this ensures a higher hit rate and also makes it so that under general conditions the number of runs increases very slightly or not at all.

III. Basic Algorithm of the Verification Subsystem

1. Since the 10 verification principles of our subsystem are by no means independent, they preserve fixed internal relationships and consequently there is also a fixed relationship between the errors they uncover individually. At the same time the degree of error positioning for the same error uncovered by certain principles also differs and consequently the efficiencies produced by different sets of ordered inspection are not the same. We did an exhaustive study of the relationships between the 10 principles and the corresponding uncovered errors and laid out a more rational, higher efficiency inspection sequence which made the algorithm simpler and wider while also speeding it up.

Separately, when the algorithm was put to use we paid equal attention to effects of the relationships between the verification principles on the data structure design and internal spacial utilization rates. As much as possible

we adopted more rational data structures according to these relationships reducing the degree of redundancy of the storage space.

The processing time of our subsystem is rather fast. In the inspection for continuity errors in a circuit network its temporal complexity analysis is as follows:

Let N_p, N_c, N_n be the number of terminal points, cell number, and network number respectively of a one level pseudo-cell description under inspection. Then the temporal complexities for each principle's inspection are:

principles i), ii), iv), and vii)	$O(N_p)$
principles iii), vi), and viii)	$O(N_c)$
principle v)	$O(N_n)$

In summary, the temporal complexity for the entire inspection is related linearly to the scale of verification objective.

Because the algorithm adopts autolocking techniques the number of runs can increase so there is a definite effect on the processing efficiency.

2. Error Localization Processing

In order to raise processing efficiency after a rational verification system discovers an error it ought not immediately terminate. Rather certain measures ought to be adopted to make it so it can continue the inspection with the result that in one run more errors can be detected and processing efficiency is raised. In our subsystem we adopted error localization methods which is to restrict the error to a localized scope preventing this kind of error from influencing the analysis and inspection of other parts. In the algorithm it is correct to take terminal points as the localization unit. When a cell code or terminal point code error occurs then it jumps that terminal point and does each inspection beginning from the next terminal point. In the algorithm sometimes cell or circuit networks are the localization unit.

IV. Experimental Results and Discussion

Our subsystem has already been used experimentally to carry out verifications with satisfying results. The experiments show that our subsystem possesses very high error recovery and error hit rates and also has very fast processing time. Of note is that the errors which were not uncovered in the experiments were all intentionally placed there by people. The other random errors were all detected for an error recovery rate of 100 percent. In addition, those few errors which the subsystem's verification principles were not able to uncover have an extremely low probability of occurring in random errors so that in general, the error recovery rate nearly reached 100 percent. For experimental results see Table 1.

1. These experimental results are result of detection of circuit network continuity errors.

Circuit Diagram Sequence		First Type Circuit			Second Type Circuit		
Circuit Scale	Number of cell types	11			17		
	Number of pseudo-cell types	2			2		
	Total number of cells	65			100		
	Total number of networks	115			224		
	Number of effective connection points	about 850			about 1,350		
Experiment Sequence		1	2	3	1	2	3
Result Data	Number of random errors	52	44	53	30	40	33
	Number of detected errors	52	44	51	29	40	32
	Error recovery rate	100%	100%	96%	96.7%	100%	97%
	Number of error information messages output	63	50	57	33	44	35
	Number of derived and pseudo errors	11	6	6	4	4	3
	Error hit rate	82.5%	88%	89.5%	87.9%	90.9%	94.3%
	Processing time (sec)	25.55	28.02	31.03	39.63	28.06	34.28

Results Without Using Autolocking Techniques

Total Number of Error Information Messages Output	88	101	100	61	87	68
Number Containing Derived or Pseudo-Errors	36	57	49	32	47	36
Error Recovery Rate	100%	100%	96.2%	96.7%	100%	97%
Error Hit Rate	59.1%	43.6%	51%	47.5%	46%	47.1%

2. Example: eight bit bidirectional shift register

number of cells	91	error recovery rate	100	percent
number of networks	113	error hit rate	100	percent
number of random errors	6	processing time	2.5	sec

Generally there are two means of connected relationship precision verification: logical simulation and heuristic verification. Generally speaking, logical simulation methods, although they are capable of more precisely outputing a waveform from a given artificial input waveform, have a low processing efficiency which gets lower as the scale of the circuit gets larger. Also error location is more difficult and usually requires human assistance. The characteristics of using heuristic principles are high processing efficiency and high degree of positionality. Moreover, the facts show, if the design is sound then the error recovery rate is completely satisfying so the method has great significance for practical engineering systems.

In the process of research on and actualization of the subsystem, colleagues of the institutes computation station provided strong support for which we specially express our gratitude.

REFERENCES

1. Gate Mark Manual, 1983.

2. Frederick J. Hill, et al., IEEE COMPUTER, 7 December 1974.

3. W. M. Vancleemput, "An Hierarchical Language for the Structural Description of Digital Systems," COMPUTER-AIDED DESIGN TOOLS FOR DIGITAL SYSTEMS, 2d Edition, 1979.

4. Zhuang Wenjun, et al., "LSIS-II Layout Design System," Third National CAD Annual Meeting, October 1985

5. Bo Jianguo, et al., "LSIS-II Hierarchical Layout Design Description Syntax and Its Compilation," Third National CAD Annual Meeting October 1985.

12,966/9599
CSO: 4008/1077

PHYSICAL SCIENCES

NEW INFRARED ABSORPTION PEAK IN HYDROGEN FZ SILICON

Beijing BANDAOTI XUEBAO [CHINESE JOURNAL OF SEMICONDUCTORS] in Chinese Vol 7 No 4, Jul 86 pp 437-440

[Article by Xuan Zhenguo [6513 2182 0948] and Zhang Meirong [1728 5019 5554] of the Emei Semiconductor Materials Research Institute and You Zhipu [3266 1807 2613] of Sichuan University Physics Department; paper received 5 May 1985]

[Text] A new Si-H absorption peak at 2,688 cm^{-1} was observed in hydrogen zone fused silicon monocrystals. This absorption peak cannot be explained by the models in references [2] and [4].

1. Introduction

The presence of hydrogen in silicon is mostly detected by infrared absorption spectra.[1,2] Infrared spectra in monocrystalline silicon are rather complex. Speaking only on the basis of the stretching vibration model, nearly 30 Si-H absorption peaks have been observed in proton injected silicon[2] and eight absorption peaks have been discovered in hydrogen zone fused silicon monocrystals.[2] In the explanation and computation of these absorption peaks there is still considerable divergence of fundamental views.[4-6] These facts demonstrate that to obtain correct understanding of states and structures of hydrogen in monocrystalline silicon will require profound experimental research.

This article reports one experimental result of our research on hydrogen zone fused silicon monocrystals: the newly observed infrared absorption peak related to hydrogen at 2,688 cm^{-1}.

II. Experimental Results

The monocrystalline silicon used in the experiments was provided by the Emei Semiconductor Material Research Institute. The resistivity of the hydrogen zoned fused monocrystal was mostly 1,000 ohms·cm and higher and at lowest 300 ohms·cm. Oxygen content was 1×10^{16}--$1 \times 10^{17} cm^{-3}$ and carbon content was 1×10^{16}--$1.6 \times 10^{17} cm^{-3}$.

We used a Perkin-Elmer 577 model infrared spectrometer at laboratory temperature to make differential spectra of the silicon monocrystal ingots. The

reference samples were high purity silicon monocrystals which had undergone multiple vacuum fusion and whose thickness was entirely the same as the observed sample, between 5 and 10 cm. The position of each absorption peak underwent correction using a Nicolet 7199B model Fourier infrared spectrometer.

1. Infrared absorption peaks of hydrogen zone fused silicon monocrystals

Measuring over 40 hydrogen zone fused silicon monocrystals, in the range of 1,900 to 2,300 cm^{-1} the eight measured absorption peaks were 2210, 2183, 2160, 2123, 2047, 1990, and 1950. These spectra did not appear at the same time in a single sample rather in each sample we were able to observe only a portion of them. Also, the relative strengths of each spectra differed according to the sample. This tallied with the results of reference [2]. In addition to these 8 spectra these experiments in 36 samples observed a previously unreported infrared absorption peak located at 2,688 cm^{-1}. A typical absorption spectra is shown in Figure 1. In the different samples the strength of the 2,688 cm^{-1} peak varies. Table 1 gives a comparison of several samples.

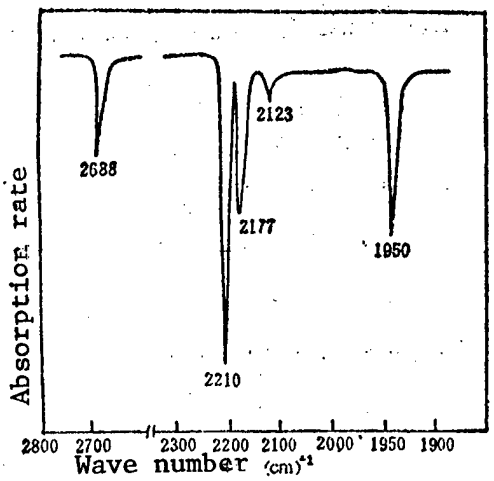

Figure 1. Infrared Absorption Peaks of Sample No 3 in Table 1 Showing a Strong 2,688 cm^{-1} Peak

Table 1. Relation of 2,688 cm^{-1} Peak to Oxygen and Carbon Content

Sample number	K_{2688}	Oxygen content $\times 10^{16} cm^{-3}$	Carbon content $\times 10^{16} cm^{-3}$
1	0.23	8.6	12.8
2	0.27	4.2	14.5
3	0.20	3.9	16.3
4	0.06	3.1	1.5
5	0.12	1.6	1.5
6	0.09	<1	<1

2. Other atmospheres

Infrared absorption spectra of silicon monocrystals

Measuring over 10 argon zone fused, vacuum zone fused, and argon vertical pulled silicon monocrystal samples, in the range from 1,800 to 3,000 cm^{-1}, we did not observe any characteristic absorption peaks.

3. Annealing features of the 2,688 cm^{-1} peak

When the samples undergo heat treatment, like the situation for known Si-H absorption peaks, the 2,688 cm^{-1} after 1 hour at 450°C begins to weaken and after annealing 2 hours at 600°C this peak vanishes together with the other Si-H infrared absorption peaks.

4. The relationship between the 2,688 cm^{-1} peak and the oxygen and carbon in the silicon

Table 1 lays out some observed test results on the relationship between the 2,688 cm^{-1} peak and the oxygen and carbon content in the silicon. Because there is no means to measure the hydrogen content, since the 2,210 cm^{-1} spectral peak is observed to be the strongest in each sample, we can only select this peak for a standard definition.

$$K_{2688} = \frac{\alpha_{2688}}{\alpha_{2210}} \tag{1}$$

To represent the relative strength of the new spectral peak in the different samples, in the formula α is the absorption coefficient of the corresponding spectral peak:

$$\alpha = \frac{1}{D} \ln \frac{I}{I_0}. \tag{2}$$

in which D is the thickness of the sample and I_0 is the base line absorption rate.

III. Discussion

1. Our experiments showed that the 2,688 cm^{-1} peak appeared only in hydrogen zoned fused silicon and that its annealing performance was the same as for the known Si-H infrared spectral peaks. This accords with the previous two major experimental bases for identifying Si-H infrared peaks [7], [2] and confirms that the newly discovered 2,688 cm^{-1} peak belongs to the Si-H infrared peaks.

2. From Table 1 we can see that in the samples with high oxygen and carbon content the 2,688 cm^{-1} peak was relatively stronger. The samples we used at the beginning were test samples that had only been zone-fused once or twice. Their oxygen and carbon contents were higher and stronger 2,688 cm^{-1} spectral

peaks were observed as shown in Figure 1. Once the position of the spectral peak is precisely known it is easy to distinguish the weaker spectral signal from the noise signal. Regular products of high resistance zone fused silicon monocrystals all have passed through several purifications and their oxygen and carbon contents are lower.[8] The previously discovered Si-H infrared spectra in hydrogen zone fused monocrystals have mostly been observed only around 2,300 cm^{-1}.[2,7,8] These two points might explain the reason why the 2,688 cm^{-1} peak had not been discovered in earlier experiments.

It ought to be pointed out that the problem of hydrogen in monocrystalline silicon is complex. For example, the oxygen and carbon contents of sample 6 in Table 1 were both below 1 x $10^{16} cm^{-3}$ but the 2,688 cm^{-1} spectral peak was still observed. Consequently, we certainly cannot reach the conclusion that this 2,688 cm^{-1} peak originates in O, C, Si-H complexes.

3. Reference [4] proposed a type of explanation for infrared absorption spectra of monocrystalline silicon containing hydrogen. They believe that in monocrystalline silicon the Si atoms on the four sides of the Si body-centered tetrahedron formed by the covalent bonds are replaced, by C, O, H, P, B, and d (representing dangling bonds) according to various combinations and each resulting configuration corresponds to an infrared absorption peak. This thinking was accepted by reference [2] and expanded but reference [6] raised objections to this model. We note that according to this model in monocrystalline silicon the corresponding structure to the infrared absorption peak with the highest wave number is (000)SiH,[4] and is located at only 2,285 cm^{-1}. The 2,688 cm^{-1} Si-H infrared absorption peak observed in our experiments obviously cannot be explained using this model.

That our experiments found a new 2,688 cm^{-1} Si-H infrared spectral peak in hydrogen zone fused silicon demonstrates that understanding of the basic structure reflected by the Si-H infrared spectral peaks in monocrystalline silicon still requires more profound experiments and theoretical research.

We are grateful to Du Yongchang of the Beijing University Physics Department for beneficial discussions and assistance.

REFERENCES

1. Picrux, S.T., Vook, F.L., and Stein, J.H., "Defects and Radiation Effects in Semiconductors," Ed. J.H. Albany, Inst. Phys. Conf. Ser. No 46, 31 (1979).

2. Cui Shufan, Mai Zhenhong, and Qian Linzhou, ZHONGGUO KEXUE [CHINESE SCIENCE] in Chinese, A, No 11, 1033 (1983).

3. Mukashev, B.N., Nussupov, M.H., and Tamendarov, M.F., PHYS. LETT., 72A, 381 (1979).

4. Shi, T.S., Shau, S.N., Oehrlen, G.S., Hiraki, A., and Corbett, J.W., PHYS. STAL. SOL., (a) 74, 329 (1982).

5. Mukashev, B.N., Nussupov, M.H., Tamendarov, M.F., and Prolov, V.V., PHYS. LETT., 87A, 376 (1982).

6. Gu Benyuan, Xu Zhengyi, and Ge Peiwen, CHINESE SCIENCE (in Chinese), A, No 1, 68 (1985).

7. Cui Shufan, Ge Peiwen, Zhao Yaqin, and Wu Lansheng, WULI XUEBAO (in Chinese), 28, 791 (1979).

8. Wang Zhengyuan and Lin Lanying, BANDAOTI XUEBAO [CHINESE JOURNAL OF SEMICONDUCTORS] (in Chinese), 3, 440 (1982).

12966/9365
CSO: 4008/1005

PHYSICAL SCIENCES

FREQUENCY MODULATION OF GaAs-$Al_xGa_{1-x}As$ DH LIGHT EMITTING DIODES

Beijing BANDAOTI XUEBAO [CHINESE JOURNAL OF SEMICONDUCTORS] in Chinese Vol 7 No 4, Jul 86 pp 450-452

[Article by Zhao Xueshu [6392 1331 1859], Li Guohua [2621 0948 5478], Wang Zhaoping [3076 0340 1627], Han Hexiang [7281 0735 4161], Shi Zhiwen [4258 1807 2429], and Wang Liming [3769 7787 2494] of the Chinese Academy of Sciences Semiconductor Research Institute and Tang Ruming [0781 3067 2494] of the Chinese Academy of Sciences Physics Research Institute; paper received 3 February 1986; first paragraph is source supplied abstract]

[Text] Abstract: This article proposes a method of using pressure for frequency modulation of semiconductor light emitting diodes, using an opposing diamond die press structure on a GaAs-$Al_xGa_{1-x}As$ DH LED we did hydrostatic pressure frequency modulation measurements (300K). Providing a seal-pad structure which was able to achieve electrical insulation, in the range of 10kbar the pressure coefficient of the LED's emission peaks was 9.8 meV/kbar and the emitted wavelength varied continuously with pressure nearly 500Å (from 8,300Å to 7,800Å).

Presently semiconductor lasers and light emitting diodes mostly use $Al_xGa_{1-x}As$ double heterojucntion (DH) structures. These structures not only possess good crystal lattice matching, at the same time they also apply restrictions on charge carriers, consequently greatly improving the light emission efficiency. Changing the X value of $Al_xGa_{1-x}As$ can change the wavelength of the emitted light satisfying various actual requirements. To insure that $Al_xGa_{1-x}As$ with source zones are located in bands, the range of change of x is $0 < x < 0.45$. Consequently, seeking lasers or LED's at different frequencies requires working from the $Al_xGa_{1-x}As$ material with different forbidden bandwidths. But the component frequencies can only be discrete and cannot realize the requirement for continuous adjustment. Even if we use an outer cavity to modulate the frequency, the adjustable range is still quite limited. This has vastly limited the applicable range of semiconductor lasers. For this reason the problem of how to achieve broadband adjustable frequency semiconductor lasers and LED's has become an important topic of current international research.

Semiconductor pressure spectral research shows that pressure can change the energy band structure of a semiconductor.[1] The effect of pressure resembles the action of changes of the constituents of an alloy. For example, static

pressure makes the Γ valley energy of GaAs rise to 10.5 meV/kbar, the energy of the L valley rise to 4.5 meV/kbar, and the energy of the X valley fall to 1.5 meV/kbar. Its effect is the same as changes in the energy band structure of $Al_xGa_{1-x}As$ with the constituents. Consequently, there is a possibility of using the pressure method to realize the goal of performing frequency modulation of semiconductor lasers and LED's. By means of changing pressure we can use a type of GaAs-$Al_xGa_{1-x}As$ DH LED (or laser) to replace all constituent $Al_xGa_{1-x}As$ components and be capable of both attaining the goals of continuity and adjustability.

To make this sort of DH LED with pressure frequency modulation possess applicability we adopted a diamond opposite corner press structure. It has a small volume, high press strength, reversibility, as well as convenient use. But the biggest shortcoming is the difficulty solving the problem of electrical insulation. At present we have not yet seen any reports concerning this aspect. Through repeated experiments we found a preliminary method to attain electrical insulation in an opposing diamond die press structure to do pressure frequency modulation of a GaAs-$Al_xGa_{1-x}As$ DH LED.

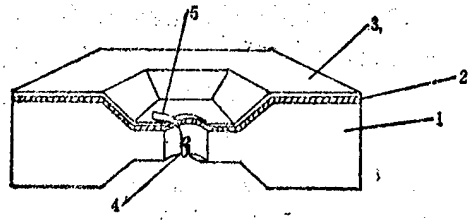

Figure 1. Pressure Frequency Modulation Structure Used in the Experiment

Key:
1. 0.5-mm stainless steel press pad acting as lower electrode
2. Dielectric insulating layer of thickness 0.1 mm using alumina ceramic
3. Steel plate 0.1 mm thick used as upper electrode
4. GaAs-$Al_xGa_{1-x}As$ DH LED
5. Diode leads

The experimental process is roughly as follows: First using a hydraulic press to compress a soft ceramic plate to an 0.15-mm thin sheet, use epoxy to glue this sheet between two metallic plates above and below. Then make an 0.5-mm hole in the center of the concavity formed by a diamond opposite corner press at a pressure of 40 kbar. This hole acts as the pressure chamber and the diode with the two electrodes above and below pressed in is inserted into the cavity with the core facing up. The original position of the installed press pad is put down on the diamond and again pressing the two diamonds makes the two metallic leads become thin sheets press bonded into the upper and lower electrodes of the press pads. Finally glycerin type solution of methanol and ethanol (4:1 by volume) is poured into the cavity. The electrically insulated closing pads can reach 30 kbar using a setup of this kind of method.

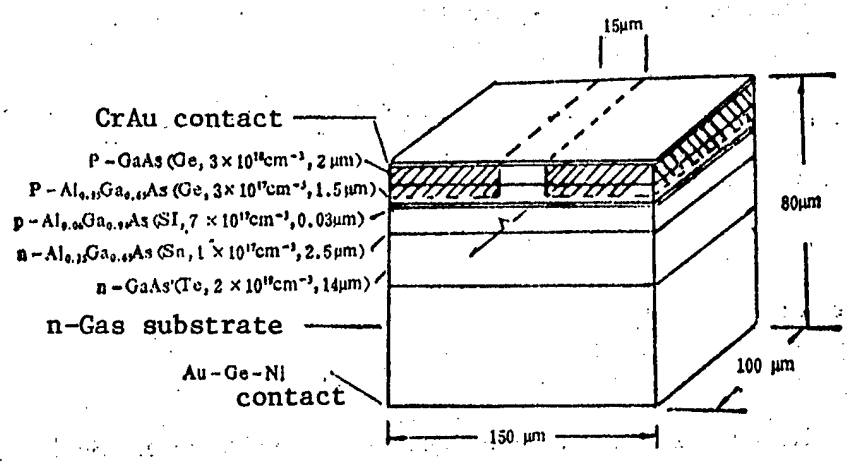

Figure 2. GaAs-$Al_xGa_{1-x}As$ DH LED Structure Used in the Experiments

Figure 2 is the structure and dimensions of the GaAs$Al_xGa_{1-x}As$ DH LED core used by the experiments from the setup of the laser research group of our institute. With an x value of 0.06 for the source $Al_xGa_{1-x}As$, under normal pressure the emitted light was 8,200-8,300Å. Figure 3 is the changing behavior of frequency with pressure measured for the LED in the range of 10 kbar using the above method. The temperature of the measurements was room temperature and the input current was 25mA. With increased pressure the energy of the emitted peaks moved higher with pressure coefficient approximately 9.8 meV/kbar and in this pressure range there was no obvious decrease seen in the intensity of emitted light. The wavelength of emitted light continuously changed about 500Å (from 8,300 to 7,800Å) and it is estimated that using this type of DH LED the effective frequency modulation range can reach 1,200Å. Presently experiments have not been done to achieve pressure frequency modulation with semiconductor lasers.

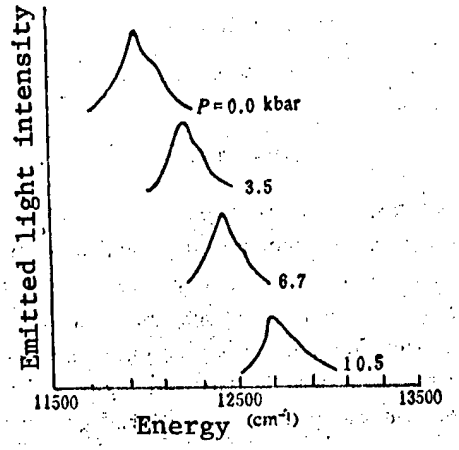

Figure 3. Movement of the Emitted Optical Peaks of the LED With Pressure Room Temperature (Input Current 25 mA)

The above preliminary research results show that it is entirely possible to use an opposing diamond die press structure to attain broadband pressure frequency modulation with respect to light emitting diodes and also to arrive at continuity, repeatability, and stability. However, at present the major problem is the lack of reliability of electrical insulation closing pads. When the pressure becomes excessive the ceramic dielectric breaks off into the cavity causing electrode short circuits. Separately, the leads of the diode in the pressurizing process experience corresponding pressures and frequently come off. These are some problems awaiting advances for resolution.

The suggestion for this topic received the enthusiastic support of our institute director, Wang Qiming, and Professors Huang Kun and He Shouan to whom we express our sincere gratitude.

REFERENCES

1. Zhao Xueshu, et al., CHINESE PHYSICS LETTER, 1 19 (1984).

2. Wolford, D.J. and Bidley, J.A., SOLID STATE COMMUN., 53 1960 (1985).

12966/9365
CSO: 4008/1005

APPLIED SCIENCES

INDUSTRIAL APPLICATIONS OF RADIOACTIVE TRACER TECHNIQUES

Shanghai HE JISHU [NUCLEAR TECHNIQUES] in Chinese No 2, Feb 86 pp 1-6

[Article by Xue Zhilun [5641 4363 4858] and Hu Xusheng [5170 1645 0524], Shanghai Nuclear Research Institute, Chinese Academy of Sciences:
"Industrial Applications of Tracer Techniques]

[Excerpt] III. Domestic Applications

Since 1958, tracer techniques have been used in industrial departments domestically and many significant results have been obtained, some of them with economic benefits which are deserving of promotion. Here we will briefly describe some tracer techniques and research results which have been made public:

1. Machine-building Industry

The Shanghai Materials Research Institute constructed a special laboratory using a reactor's integral radioactivation analysis technique to carry out abrasion research on piston rings, lubricating oil, and oil injection precise needle valves, for example the precision of measuring the latter can reach a magnitude of 10^{-7}g.

The Shanghai Nuclear Research Institute used a proton beam produced by a cyclotron to carry out work on thin layer radioactivation method measurement of machine part abrasion, and to carry on experimental research on the amount of abrasion and abrasion erosion on 240 mm piston rings electrosprayed with pure molybdenum in East Wing internal combustion engine and a 12.7 mm gun barrel, with significant results. For example, in measurement of the latter, the sensitivity and precision were more or less the same as the results provided by the U.S. Army Ballistics Research Institute.

2. Metallurgy Industry

Domestically, work in this area began very early and there have been more results.

a. Application of tracer atoms in ore selection. Beginning in 1959 the Ore Smelting Institute of the Ministry of Geology and Natural Resources synthesized radioactive yellow powder a necessary flotation agent and

carried out research on its application in non-ferrous sulfide ore and rare metal ore flotation. ^{35}S was used to synthesize radioactive yellow powder and ^{32}P was used to synthesize radioactive ethyl sodium yellow powder and the theory and mechanism of flotation were explored.

b. Role of rare earth elements in the iron and steel industry. The Beijing Iron and Steel Institute's Physical Chemistry Teaching and Research Group used ^{141}Ce as a tracer to study the behavior of rare earth elements after entering molten iron. They also used ^{141}Ce to study the diffusion coefficient, diffusion excitation energy and D_o value of cerium in iron in the 800-1100°C range and felt that in addition to having a purifying role when added to steel, rare earth elements also have an alloying role.

c. Others. The Ministry of Metallurgy's Iron and Steel Institute used radioisotopes of ^{60}Co as a tracer atom to study the diffusion of cobalt in precipitation hardened nickel-base cast alloy, and thus explored the strengthening function of Al and Ti on nickel-base cast alloys. Electroslag smelting cast purified alloys are generally acknowledged, especially the results of eliminating non-metallic contaminants. They used $^{95}ZrO_2$ tracers to study the direction of oxidized physical contaminants represented by ZrO_2 in alloys and steel in the electroslag smelting process.

3. Electronics Industry

The ^{85}Kr leak detection technique has been applied domestically. Cooperative research of Fudan University and the Shanghai Electron Components No 5 Plant resulted in an ^{85}Kr leakage detection method which is suitable for small scale components sealed in metal, ceramics or glass, such as transistors and integrated circuits. It has the advantages of high sensitivity, high detection speed and ease of operation.

4. Petroleum Industry

Radioactive tracer technology has been applied to oil well measurement work. In 1982, China injected an activated rock carrier with ^{131}I as the radioactive tracer into 161 water injection wells then measured the volume of water injected into each small stratum of the oil-producing stratum section. The Daqing Oil Field used this method to clarify the water absorption ability of water injection wells, determined the volume of water injected then extracted oil by strata and injected water by strata with clear economic results.

The Shengli Oil Field forced a ^{65}Zn radioactive tracer liquid into the strata to check the channels on the outside of the oil well pipe and this method was widely adopted in this oil field with good results.

The Shanghai Nuclear Research Institute cooperated with relevant units to research a radioisotope underground oil tube leak detector. ^{131}I tracer oil was passed through the tube and by passing the leak detector through the oil tube channels the location of oil tube leaks could be determined. This technique was tested at four airfields and oil stations and found a

total of seven leaks of various sizes. Compared with excavation to find leaks, using this leak detection technique can save a great deal of manpower and material and taking into consideration that this method can avoid the waste involved in recklessly exchanging new pipelines, then the economic benefits are clear. This institute developed a new high performance leak detector which can be used on longer distances and larger pipelines and it is now in trial use.

5. Water Conservancy Engineering

Isotope tracer technology has been applied in a preliminary way to controlling the Huang He. For example, by using radioisotope ^{113m}In absorbed in the surface of silt grains it is possible to accurately measure the sedimentation rate of silt of different granularity in turbulent water and good results have been obtained. Or ^{169}Yb as a tracer has been used for measuring the flow of the Huang He.

Tracer technology has also played an important role in reservoir embankment imperviousness and harbor navigation channel dredging and demonstrated its superiority. Beginning in 1974, the Nanjing Water Conservancy Sciences Institute used isotope tracer technology to complete observation missions on four defective and dnagerous reservoir embankment leaks and obtained definite results. For example, the Longhekou Reservoir in Anhui was ranked as the most dangerous reservoir in the province. The measurement data obtained by the instittue using $Na^{151}I$ tracer technique indicated that a contact washout or pipe leak could not occur in the embankment and that it did not require imperviousness strengthening but only that the covered cracks on the front of the embankment be filled in and the water level could be raised, thus saving the province several million yuan for imperviousness strengthening.

For the past few decades the silting in the harbor and navigation channels of Zhenjiangkang have become more serious daily, and each year over 1 million yuan is spent dredging the harbor and navigation channels so that they can maintain an effective depth of 4 meters. The Nanjing Water Conservancy Sciences Institute used radioactive ^{46}Sc to manufacture a tracer silt to place on the river bottom and successfully observed the movement of sand in shoals, clarified the movement direction and discovered an important source of the silt deposits in the Zhenjianggang area, which played an active role in harbor and navigation channel construction.

IV. Conclusion

From the above, one can see that radioactive tracer technology is not a very complicated and expensive technique. Ordinary laboratories and plants have the conditions for carrying on research and application in this area. The expenses required for application basically only involve equipment for radioisotopes and tracer synthesis, training of operating personnel, and allocation of some necessary small nuclear measuring instruments, while the economic benefits obtained from applying this technique are enormous. At present the trend internationally is how to perfect this technique, open more application areas, and obtain even higher economic benefits.

In China, industrial applications of radioisotope tracer technique has a good foundation and is not getting started too late, but in terms of the scale and range of applications, it is still clearly not enough and thus the potential is still very great. We believe that if only the relevant sections would place some stress on it, reorganized and supplement research forces, and adopt a series of urgent measures, it will be possible to accelerate China's application of radioactive tracer technique. While promoting radioisotope knowledge and ensuring safety, the nation should encourage relevant industrial sections and scientific research sections to apply this technique vigorously to resolve the major actual problems in production and scientific research in this way we will accumulate more application experience and obtain even more delightful economic benefits.

REFERENCES

[1] INDUSTRIAL APPLICATION OF RADIOISOTOPES AND RADIATION TECHNOLOGY, IAEA Proceedings Series, Vienna, 1982.

[2] G.R. Choppin and J. Rydberg, NUCLEAR CHEMISTRY--THEORY AND APPLICATION, Pergamon Press, 1980.

[3] P. Daudel, RADIOACTIVE TRACERS IN CHEMISTRY AND INDUSTRY, Charles Griffin & Co. Ltd., London, 1960.

[4] J.J. McMahon and A. Berman, INDUSTRIAL USES OF RADIOISOTOPES, National Industrial Conference Board, Inc., 1958.

[5] TONGWEISU ZAI GONGYESHANGE YINGYONG [APPLICATION OF ISOTOPES IN INDUSTRY], Haerbin Huiyi Ziliao [Harbin Conference Materials], Sep 1977.

[6] FANGSHEXING TONGWEISU YU SHEXIAN YINGYONG ZHANLANHUI ZILIAO [RADIOACTIVE ISOTOPE AND RAY APPLICATION EXHIBIT MATERIALS], Beijing, April 1972.

8226/9835
CSO: 4008/75

APPLIED SCIENCES

LARGE FERRITE CORE TESTS USING A 50ns PULSE

Chongqing HEJUBIAN YU DENGLIZITI WULI [NUCLEAR FUSION AND PLASMA PHYSICS] in Chinese Vol 5 No 4, Dec 85 pp 224-227

[Article by Cheng Nianan [4453 1819 1344], Liu Chengjun [0491 2110 0193], Dai Guangsen [2071 0342 2773], Zhang Shouyun [1728 1108 0061], and Tao Zucong [7118 4436 5115]]

[Text] Abstract. This article describes experiments with a large ferrite core using a 50 ns pulse. The core's outer diameter was 50 cm, the inner diameter was 20-25 cm, and the thickness was 2.5 cm. It provides the voltage and excitation current of the ferrite core and the reset current waveform as well as the ΔB vs ΔH curve of typical pulses. When the pulse reset field peak value is 2-4 Oe we get flux amplitudes $\Delta B > 0.7$ T and incremental magnetic permeability $\mu \sim 400$.

Keywords: Ferrite core, flux amplitude, incremental magnetic permeability, linear induction accelerator.

I. Introduction

Ferrite used as the magnetic material for a linear induction accelerator has many advantages[1]. The working principles of this sort of accelerator can be illustrated by Figure 1. The ferrite ring actually constitutes a single turn pulse transformer. When the high voltage pulse produced by the pulse forming network goes through the switch into the primary it causes changes in the magnetic flux inside the ferrite ring. Consequently in the accelerating gaps at the two ends of the secondary an axially directed accelerating electric field is induced. The volt-sec value of the accelerating voltage is determined by the pulse characteristics and the transverse area of the ferrite ring. According to Faraday's law the accelerating voltage is

$$u(t) = -S\frac{dB}{dt} \qquad (1)$$

in which S is the transverse area of the ferrite ring.

The part of the ferrite ring structure which produces this accelerating voltage is called the accelerator cavity. Figure 2 is a schematic of the

cross section of a typical accelerator cavity. In order to increase the accelerating voltage many ferrite rings are placed in the cavity. Usually an accelerator cavity can produce accelerating voltages with flat voltages of several hundred thousand volts and half height widths of several tens of nanoseconds. Accelerator cavities generally use Blumlein transmission lines to provide pulsed high voltage and Blumlein lines use Marx generator or harmonic transformer current.

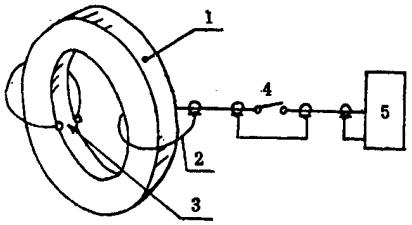

Figure 1. Principles of a Linear Induction Accelerator

Key:

1. Ferrite ring
2. Primary
3. Accelerator gap [secondary]
4. Switch
5. Pulse forming network

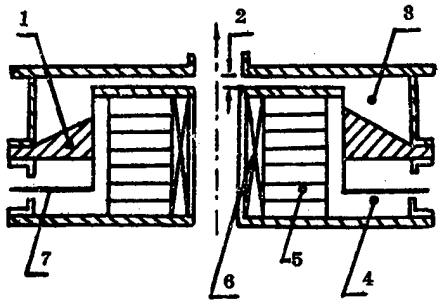

Figure 2. Cross Section of an Accelerator Cavity

Key:

1. Insulator
2. Accelerating gap
3. Vacuum
4. Oil
5. Ferrite ring
6. Focusing solenoid
7. Input point for high voltage pulse

In this sort of application, the ferrite acts first as an energy transmission medium. Consequently the requirements for the ferrite are: 1) large flux amplitude ΔB to capture a high accelerating voltage volt-sec value; 2) large incremental magnetic permeability μ_Δ to get a high rate of energy transmission efficiency; 3) small coercive strength H_c to facilitate reset; and 4) large resistivity ρ for high insulation strength.

Next the ferrite acts as a kind of energy absorption medium. It ought to be able effectively to absorb high frequency (in the range of 10^9 Hz) transient voltages induced when the beam passes through the accelerator cavity to prevent them from interfering with the accelerating voltage and energy supply system.

When evaluating and selecting ferrite material for use in a linear induction accelerator tests must be done with regard to the ΔB vs ΔH curve of the ferrite ring pulse. In order to get useful results these kind of tests must be carried out with a ferrite ring as much as possible under reset and

excitation conditions approximating accelerator operation with nearly real dimensions[1].

II. Test Apparatus

In order to simulate reset and excitation conditions of linear induction accelerator operation we set up the test apparatus shown in Figure 3. The pulse forming network use plane water medium Blumlein lines, pulse width was τ = 50 ns, and the simple root characteristic impedance was $Z_0 = 4.12\Omega$. The plane Blumlein lines use Marx generator current. The impulse capacitance C_M and equivalent inductance L_M can be adjusted based on the test requirements. The ferrite cavity is a coaxial single turn coil. Crossing a small coaxial transition section it connects with the plane Blumlein line. The dimensions of the ferrite ring to be tested were: outer diameter 50 cm, inner diameter 20-25 cm, and thickness 2.5 cm. In order to avoid voltage doubling in the coaxial transition section two compensating resistors were placed symmetrically. The magnitude of the resistances can be adjusted.

The equivalent circuit of the Marx generator, plane Blumlein line, and ferrite cavity is as shown in Figure 4. From the figure it can be seen that when the Marx generator gives a charge to the Blumlein line a small portion counter flow of the charging current passes to the ferrite cavity reseting the ferrite. When the Blumlein line operates it provides the ferrite cavity with a nearly square voltage pulse to make the ferrite ring produce a pulsed magnetization.

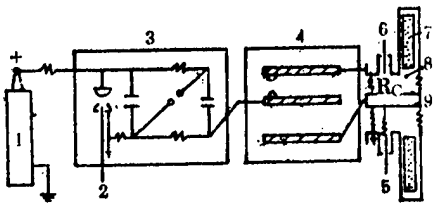

Figure 3. Test Apparatus

Key:

1. DC current source
2. Trigger input
3. Marx generator (when testing multiple rings changed to five stages)
4. 50 ns, 4.12 ohm plane water medium Blumlein line
5. Resistance voltage divider
6. Capacitance tanji
7. Ferrite ring
8. Oil
9. Resistance current divider

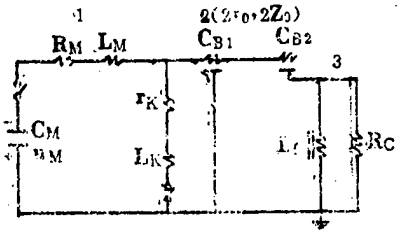

Figure 4. Circuit Model of Marx Generator, Plane Blumlein Lines, and Ferrite Cavity

Key:

1. Marx generator: C_M impulse capacitance, L_M equivalent inductance, R_M equivalent resistance (including switch resistance)
2. Blumlein line: Z_0 simple root line characteristic impedance, τ_0 simple root line electrical length, C_{B1} and C_{B2} respectively capacitance between upper and middle and middle and lower plates; r_k switch resistance, L_k switch inductance
3. Ferrite cavity: L_f ferrite cavity inductance, R_c compensation resistance

In order to determine the pulse ΔB vs ΔH curve, we use the resistance voltage divider and capacitance tanji to measure the voltage of the ferrite cavity and use the resister current divider to measure current flowing through the ferrite cavity in the reset and excitation interval. Separately readings are done with respect to the charging voltage and charging current of the Blumlein line. To prevent interference all the measuring instruments are put in a shielded room.

Experiments show that this testing apparatus can provide excitation voltage pulses with pulse reset fields (reset interval variable from 1.4 to 2 μs) with peak values of around 4-5 Oe and rise time of 7 ns, half height widths of 55 ns, and maximum flat voltages approaching 300 kV. This apparatus can be used in single ferrite ring tests and can also be used in multiple ring tests.

III. Test Results and Discussion

When the ferrite ring has not reached saturation the typical waveform of the reset current, and excitation current and voltage is as shown in Figure 5. From the figure it is evident that the peak reset current is 260 A and the reset interval is 1.4 μs. The voltage waveform is extremely close to a square wave and the flat amplitude value is 37 kV, the rise time 11 ns (subtracting the divider and oscilloscope rise time, actually 8 ns), and half height width is 55 ns. That the peak excitation current is 980 A and is nearly a straight line in most of the region shows that during the pulse magnetization interval the ferrite ring is basically a linear inductor.

When calculating the pulse ΔB vs ΔH curve, the flux amplitude ΔB is gotten according to formula (1) by integrating with respect to the ferrite cavity

voltage u(t). The integral is computed by using the trapezoidal method or using an RC integrator to integrate the u(t) signal directly. The corresponding ΔH is obtained directly from the excitation current waveform. The incremental magnetic permeability μ_Δ is defined as ratio of the ΔB and ΔH values at the end points of the pulse ΔB vs ΔH and represents the average magnetic permeability during the pulse excitation interval.

Figure 5. Voltage and Current Waveforms for a Single Ferrite Ring (C_5)

a) Reset current waveform. Vertical axis 83.2 A/square, horizontal axis 0.5 s/square
b) Voltage (1) and excitation current (2) waveform. Time standard 10 ns.

Figure 6 gives representative pulse ΔB vs ΔH curves for various type ferrites. These curves were obtained under a peak value reset field of 2 - 4 Oe. From the figure we see that for rings with good pulse properties, such as C_5, under a reset field of 2.8 Oe we get $\Delta B = 0.61$ T, $\mu_\Delta = 591$, and a single ring volt-sec value approaching 1.94 mV·s moreover saturation has not been reached. Pulse properties are lacking in some rings, like C_4. μ_Δ is only around 300 and the necessary peak excitation current is too high. This is not desirable.

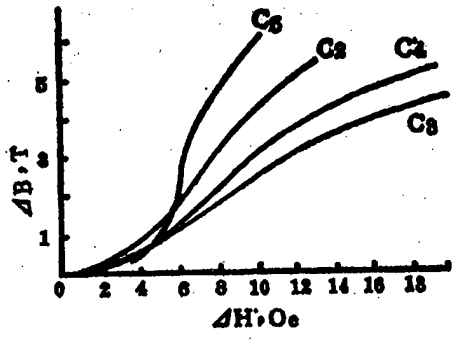

Figure 6. 50 ns Pulse ΔB vs ΔH Curves for Different Ferrite Rings

In order to utilize completely the flux amplitude that the ferrite ring can obtain the selection of reset conditions and pulse excitation initial conditions is extremely important. When the ferrite ring resets from B_r to $-B_r$, that is when the initial magnetic state is selected as $-B_r$ for the pulse excitation, the maximum flux amplitude that can be reached is $\Delta B = B_s + B_r$, B_s and B_r respectively being the saturation flux density and the remainder flux density of the ferrite ring. But when the initial magnetic state is selected near $-B_s$, the maximum ΔB can tend to $2B_s$. This makes the obtained

ΔB obviously higher. In order to achieve this sort of requirement, as can easily be seen in Figure 4, it is necessary to adjust appropriately the size of the charging time and charging current provided to the Blumlein line from the Marx generator as well as the size of the compensating inductance R_c to keep the ferrite ring at the saturation state for the reset direction when the Blumlein line charging voltage reaches its peak value. During the tests we used this technique and also established corresponding simulation computation methods which took into account the non-linearity of the ferrite ring. Computations and test results were basically in agreement.

For comparison, Figure 7 gives the pulse ΔB vs ΔH curve for a C_1 ring and corresponding curve under 50 Hz. The rate of change of the curve under 50 ns in the figure is even because in the pulse magnetization process the change in magnetic density B in the time interval always lags behind the change in magnetic field strength H. The tests show that under 50 Hz, for rings with high B_s and B_r and small H_c the general pulse properties were also better.

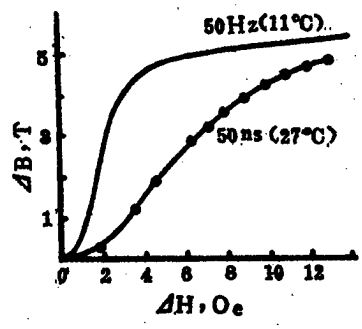

Peak Value Reset Field 4 Oe

Figure 7. 50 ns and 50 Hz B vs H curves for C_1 Ferrite Rings

On the basis of single ring experiments we performed multiple ring experiments. These experiments prove the volt-sec values of multiple rings fundamentally are the sum of the individual ring volt-sec values. Figure 8 is the voltage waveform from a seven ring experiment with a basic rise time of 14 ns, half height width 55 ns, and flat voltage of 352 kV. This is equal to each ring's ΔB = 0.72 T and μ_Δ = 450.

Vertical axis 174 kV/square, horizontal axis 20 ns/square

Figure 8. Seven Ring Experiment Voltage Waveform

The experiments already done show that the test apparatus operation is reliable and the maximum test errors in voltage and current are about ±5 percent. The test results provide a reliable basis for selection of the composition and processing of the ferrite.

Also participating in the work were Pan Shicheng, Yao Yibing, and Shi Shangchun to whom we express our special thanks here.

REFERENCES

1. Reginato, L., et al., UCRL-00811, 1978, pp 1-3.

12,966/9599
CSO: 4008/6

Acoustics

COMPUTER SIMULATION OF DIRECTIVITY OF DIGITAL MULTI-LAYER, MULTI-BEAM SYSTEM

Beijing YINGYONG SHENGXUE [APPLIED ACOUSTICS] in Chinese Vol 5, No 3, Jul 86 pp 17-22

[Article by Li Qihu [2621 0796 5706] and Xiang Dingchang [7309 1353 7022] of Institute of Acoustics, Chinese Academy of Sciences; and Lu Xiaoyan [0712 1420 3601] and Dong Li [5516 3769/0448] of China Shipbuilding Industry General Corporation]

[Abstract] Multi-beam formation with the action of a lateral-direction filter is a way of new beam formation in digital sonar. The directivity of this system is related to sampling frequency quantizing errors, the layered bit number, and time-delay compensation. The deviation between the actual directional characteristic of the system and the ideal steady-state characteristic will directly affect properties of the sonar. The paper derives various equations needed to calculate directivity of this system. At the same time, a system simulation was performed on a computer. The simulation result can provide evidence for the selection of some parameters of digital sonars. Four tables list data showing the effect on directivity due to the number of elements and the operational sector, the effect on main-lobe response due to time quantization, and ways of combining amplitude (and time) quantization and integration time. Eight figures show diagrams of multi-beams formed with the action of a lateral-direction filter, calculation of directivity of the circular-arc array, two methods of analog-to-digital conversion, and effects on directivity due to the number of elements, operational sector, integration time, and quantization of amplitude and time. The authors are grateful to Liang Zuwei [2733 4371 1218] and Ren Hao [0117 3185] for their assistance in the system simulation. The paper was received for publication on 5 May 1983.

10424/9835
CSO: 4009/107

EFFECT OF PIEZOELECTRIC COUPLING FACTOR AND COMPLEX IMPEDANCE ON IMPULSE RESPONSE OF A PIEZOELECTRIC TRANSDUCER

Beijing YINGYONG SHENGXUE [APPLIED ACOUSTICS] in Chinese Vol 5, No 3, Jul 86 pp 30-34, 29

[Article by Zhou Tieying [0719 6993 5391] of Department of Physics, Qinghua University; Wei Jianxin [7614 1696 2450] of Institute of Petroleum Physical Prospecting, Ministry of Geology and Mining; and Qian Deping [6929 1795 1627] of Graduate Student Division, Wuhan Geology College]

[Abstract] In seismic modeling experiments, a low-frequency piezoelectric transducer of uniform directivity and short pulse persistence time is required. Found experimentally, the video frequency period of the transmitted pulse of the transducer with matched line is always longer than that without a matched line. The pulsed waveform is more complex if radiated into water rather than onto a slender rod. However, thus far these phenomena have not been explained in detail.

Starting from the fundamental piezoelectric equation and Mason equivalent circuit, the paper computes the transfer functions of a length mode piezoelectric transducer, the prime-mover-to-generator coupling coefficient by a numerical method; and the effect that the complex impedance has on the pulsed waveform of a length mode piezoelectric transducer. Shown by results, the greater the coupling coefficient of the transducer with a matched line, the wider the monopolar pulse width; the pulsed waveform becomes complex owing to the complex impedance. The authors conducted experiments on the effect that the complex impedance has on the pulsed waveform; results from calculations and experiments are in basic agreement. Under certain approximate conditions, these results serve as reference data in designing and operating pulsed piezoelectric transducers. Nine figures show a rod-shaped transducer and the Mason equivalent circuit; effects of the coupling coefficient on the transducer function, monopole pulse width, and pulsed waveform; curves of piston impedance function; effect of complex impedance on radiation pulse waveform; and acoustic waveforms. The authors are grateful to researcher Zhu Guozhen [6175 0948 2823] of Acoustics Laboratory of Qinghua University, and associate researcher Li Mingxian [2621 2494 6513] of Institute of Acoustics, Chinese Academy of Sciences for their assistance. The paper was received for publication on 8 November 1984.

10424/9835
CSO: 4009/107

MEASUREMENT OF SAW VELOCITY USING KNIFE-EDGE TECHNIQUE

Beijing YINGYONG SHENGXUE [APPLIED ACOUSTICS] in Chinese Vol 5, No 3, Jul 86 pp 39-41

[Article by Gan Changming [1626 2490 2494] of Acoustics Institute, Nanjing University]

[Abstract] This paper describes a method of using a laser probe (knife-edge technique) to determine SAW velocity; SAW stands for surface acoustic wave. This method was used to determine the SAW velocities of free surfaces of Y-cut, X-propagation quartz crystal chips and metallized surfaces. Applying the coherence property of excited and received signals, the authors constructed a simple interference system capable of measuring SAW phase velocity. An ordinary measuring microscope is used as the moving attachment; after wave detection with the received signals, a double-pen x-y plotter serves in recording. Wavelength is thus measured from plotted curves thereby avoiding human error in readings. The phase velocity accuracy is higher than 0.1 percent; the wavelength accuracy is about 0.4 percent.

One table lists measured SAW velocity data. Four figures show a SAW velocity measurement arrangement, plots of interference signals, structure of a specimen used for SAW velocity measurement, and diagrams explaining the principle of generating deviations. The author is grateful to Yu Jiong [6735 8741] and Li Youzhi [2621 2589 1807] for providing specimens for experiments. The paper was received for publication on 31 January 1984.

10424/9835
CSO: 4009/107

JPRS-CST-86-050
28 November 1986

COMPUTER-AIDED CALCULATED COMPOSITION OF MOTHER LIQUOR IN THE HOU DEBANG PROCESS FOR MAKING SODA

Shanghai HUAXUE SHIJIE [CHEMICAL WORLD] in Chinese No 7, 25 Jul 86 pp 310-313

[Article by Wang Jirong [3769 1015 6954] and Zhang Mousen [1728 8574 2773] of China University of Science and Technology]

[Abstract] Dr Hou Debang [0186 1795 2831] invented the Hou process for making soda; the process is also called the joint soda manufacture process, using the technical process of one salt addition, two ammonia absorptions, and one carbonization operation. To control the production process, the composition and variation rule of the soda solution (also called mother liquor I) exiting the carbonization tower should be mastered. In a book by Hou, ZHIJIAN GONGXUE [ENGINEERING IN SODA MANUFACTURE], this problem is illustrated in an entire chapter; he listed seven simultaneous equations, which were solved by Hou using the method of successive approximations. This paper proposes a numerical method (different from Hou's calculation scheme) for solution with a computer. Only one minute is required from the time of data input to printout as tested on a DP-32 microcomputer. There are 31 lines (program) written in BASIC language. A table lists the results of Hou's calculations and the computer output; the two results are in agreement. One figure shows a flowchart of the computer program.

REFERENCES

[1] Hou Debang, ZHIJIAN GONGXUE, Chemical Industry Publishing House, Beijing, 607, 611 (1960).

[2] Dalian Chemical Works, LIANHEFA SHENGCHAN CHUNJIAN HE LUHUA'AN [PRODUCTION OF SODA ASH AND AMMONIUM CHLORIDE BY THE JOINT SODA MANUFACTURE PROCESS], Petrochemical Industry Publishing House, Beijing, 94 (1977).

[3] Dalian Institute of Soda Manufacture Industry, LIANJIAN SHENGCHAN FENXI FANGFA [ANALYSIS METHOD ON JOINT SODA MANUFACTURE], Petrochemical Industry Publishing House, Beijing, 94 (1977).

10424/9835
CSO: 4009/1110

Biochemistry

DNA SEGMENTS OF Bm SNPV WITH NUCLEUS GENE INITIATOR ACTIVITY

Beijing ZHONGGUO KEXUE (B JI) [SCIENTIA SINICA: SERIES B (CHEMICAL, BIOLOGICAL, AGRICULTURAL, MEDICAL & EARTH SCIENCES)] in Chinese No 4, 1986 pp 389-395

[Article by Xin Jihou [1823 4764 0624], Gu Maozhi [7357 2021 3112], Wang Heng [3769 3801], Li Mintang [2621 2404 2768], and Li Zaiping [2621 6528 1627] of Shanghai Institute of Biochemistry, Chinese Academy of Sciences; Li Honghua [2621 3163 5478] of Shandong Agricultural College; and Zhou Jintao [0719 6855 3447] of First Shanghai Municipal Medical College]

[Abstract] The cloned plasmid pHE5 of bacillus coli initiator was employed to clone and isolate eight kinds of HindIII enzyme solute DNA segments and one kind of SaII enzyme solute DNA segment of Bm SNPV (Bombyx mori L. silkworm nucleus polygonal virus) gene sector. The authors discovered that these DNA segments can direct the initiator activity expressed by the anti-tetracycline gene. These segments also determine the anti-tetracycline capacity of strains of recombination plasmids at a concentration of these DNA segments. The highest capacity among these DNA segments in resisting tetracycline exists approximately 30 μg/ml. The authors analyzed a fragment of the nucleotide sequence of a DNA segment, discovering a sequence structure very similar to the nucleating gene initiator. One table lists the properties of DNA segments with Bm SNPV initiator activity, a comparison between the Bm SNPV DNA sequence with initiator activity and its nucleating initiator, electrophoresis digrams of enzyme solute products, and growth of recombination plasmid strains in different concentrations of tetracycline. The authors are grateful to the following colleagues: Zhu Shengzu [2612 4939 4371] and Cai Mingjie [5591 0682 2638] for preparation of HingIII and SaII enzymes, and Ao Shizhou [2407 0013 3166] for providing plasmic pHE5 DNA and for advice. The first draft of the paper was received on 3 April 1984; the revised draft was received for publication on 3 November 1985.

REFERENCES

1. Wast, R. W., et al., GENE, 9 (1979), pp 271-288.
2. Ao Shizhou, et al., YIZHUAN XUEBAO [HEREDITY JOURNAL], 10 (1983), pp 85-90.

3. Neve, R. L., et al., NATURE, 277 (1979), pp 324-325.

4. Mitsialis, S. A., et al., GENE, 16 (1981), pp 217-225.

5. Jenkins, F. J., et al., J. VIROL., 45 (1983), pp 478-481.

6. Mcknight, T. D., and Meagher, R. B., ibid., 37 (1981), pp 673-682.

7. Wu Xiangfu [0702 4382 3940], et al., YIZHUAN XUEBAO, 10 (1983), pp 175-179.

8. Messing, J., and Vieira, J., GENE, 19 (1982), p 269.

9. Birnooim, H. C., et al., NUCLEIC ACIDS RES., 7 (1979), pp 1,513-1,523.

10. Xin Jihou [1823 4764 0624], ZHONGGUO KEXUE (B JI), 1984, 9: pp 805-810.

11. Hereditism Project Section, Laboratory No 7, Shanghai Institute of Biochemistry, Chinese Academy of Sciences, SHENGWU HUAXUE YU SHENGWU WULI XUEBAO [JOURNAL OF BIOCHEMISTRY AND BIOPHYSICS], 11 (1979), pp 215-222.

12. Dretzen, G., et al., ANAL. BIOCHEM., 112 (1981), pp 295-298.

13. Maxam, A. M., and Gilbert, W., METH. ENZYM., 65 (1980), pp 499-560.

14. Wang Heng [3769 3801], et al., ZHONGGUO KEXUE (B JI), 1985, 9: pp 245-251.

15. Hans-Henrik, M., DAHL TIBS JULY, 1983, p 230.

16. Onoderd, K., et al., J. MOL. BIOL., 13 (1965), p 532.

17. Cohen, J.D., et al., PROC. NATL. ACAD., SCI., USA, 77 (1980), pp 1,078-1,082.

10,424/9599
CSO: 4009/1083

STUDY OF SELENIUM AND RED BLOOD CELLS

Beijing ZHONGGUO KEXUE (B JI) [SCIENTIA SINICA: SERIES B (CHEMICAL, BIOLOGICAL, AGRICULTURAL, MEDICAL & EARTH SCIENCES)] in Chinese No 4, 1986 pp 396-406

[Article by Yang Fuyu [2799 4395 1938] and Wo Weihan [3087 4850 3352] of Institute of Biophysics, Chinese Academy of Sciences]

[Abstract] This paper is presented in two parts: (I) Effect of selenium on Na, K-ATP enzyme activity and fluidity of red blood cell, and (II) red blood cell protective function of selenium.

The selenium content in human red blood cells can affect the structure and function of the cell membrane. Reduced selenium content will lower the K-ATP enzyme activity and fluidity of membrane fat. By adding traces of Na_2 SeO_3 (0.03 to 0.3 ppm Se), the Na, K-ATP enzyme activity and membrane-fat fluidity can be significantly increased. More than half an hour of pre-treatment should be conducted on red blood cell membranes using selenium in order to achieve the apparent effect.

Selenium's protective function for red-blood-cell membranes is generally explained as due to activity of Se-GSHPx; however, GSHPx is mainly distributed in red-blood-cell cytoplasm. Therefore, the phenomenon of the apparent protective function to cell membranes exerted by the combination of red blood cells and selenium appears to be very difficult to account for by the function of GSHPx.

In Part I, two tables list comparative data on selenium levels, Na, K-ATP enzyme activity, and DPH fluorescence polarization; and the effect on enzyme activity and polarization due to different amounts of selenium. Three figures show selenium's effect on Na, K-ATP enzyme activity and DPH fluorescence polarization, and the relationship between Na, K-ATP enzyme activity and the duration of pre-treatment using red blood cells and selenium.

In Part II, four tables list data comparing increased DPH fluorescence polarization, and comparing GSHPx activity, comparison between enzyme activity and DPH fluorescence polarization, and electrophoresis spectrograms of the residual spectrin gel on red-blood-cell membrane. Four figures show the aging time versus the inhibited percentage due to ouabain in isolated red blood

cells, an electrophoresis scanning spectrogram of the SDS-polypropene acylamine gradient gel, a spectrogram showing selenium's effect on red blood cell aging, and a spectrum showing the difference in reactions with DTNB after aging with or without selenium.

The first draft of the paper was received on 22 November 1984; the revised draft was received for publication on 5 April 1985.

REFERENCES (for Part I)

1. Shamberger, R. J., BIOCHEMISTRY OF SELENIUM (Ed. Frieden, E.), Plenum Press, New York and London, 1983, pp 31-54.

2. Shamberger, R. J., ibid., Plenum Press, New York and London, 1983, pp 225-227.

3. Shamberger, R. J., ibid., Plenum Press, New York and London, 1983, p v.

4. Yang Guangqi [2799 0342 0967], "Third International Symposium on Selenium in Biology and Medicine," Beijing, 1984.

5. Tan Jianan [6223 6015 1344], ibid., Beijing, 1984.

6. Wang Fan [3769 0416], ibid., Beijing, 1984.

7. Li Chongzheng [2621 1504 2973], et al., ibid., Beijing, 1984.

8. Xi Guangzheng [1153 0342 1073], et al., ibid., Beijing, 1984.

9. Li Fangsheng [2621 5364 3932], et al., ibid., Beijing, 1984.

10. Guo Shusen [6753 2885 2773], et al., "Collected Papers at the Third All China Keshan Disease Pathology and Pathogenesis Symposium," 1982, p 13.

11. Wang Keli [2769 0344 4409], et al., "Collected Papers at the Third All China Keshan Disease Pathology and Pathogenesis Symposium," 1982, p 16.

12. Yang Tongshu [2799 0681 2579], et al., "Collected Papers at the Third All China Keshan Disease Pathology and Pathogenesis Symposium," 1982, p 45.

13. Schwarz, K., et al., J. BIOL. CHEM., 235 (1960), pp 3,387-3,392.

14. Wu, S. H., et al., BIOL. REPROD., 20 (1973), pp 793-798.

15. F. Y. Yang (Yang Fuyu), et al., "Third International Symposium on Selenium in Biology and Medicine," Beijing, 1984.

16. Wo Weihan [3087 4850 3352] and Yang Fuyu, ZHONGGUO KEXUE (B JI), 1986, 4: pp 401-406.

17. Zwaal, R. A. Z., et al., BIOCHEMICAL ANALYSIS OF MEMBRANE (Ed. Maddy, A. H.), Halsted Press, New York, 1976, pp 371-373.

18. Pearson, T. W., et al., LIFE SCIENCE, 22 (1978), p 127.

19. Shinitzky, M., et al., BIOCHEM. BIOPHYS. ACTA, 515 (1978), p 367.

20. Warburg, O., et al., BIOCHEM. Z., 40 (1939), p 303.

21. Holker, J. R., et al., J. APPL. CHEM., 8 (1958), pp 1-3.

22. Jenkins, K. J., et al., CAN. J. BIOCHEM., 49 (1971), pp 468-472.

23. Kirkpatrick, F. H., LIFE SCIENCES, 19 (1976), pp 1-18.

24. Yang Fuyu, et al., ZHONGGUO KEXUE (B JI), 1983, 6: pp 519-527.

25. F. Y. Yang (Yang Fuyu), et al., BIOCHEM. BIOPHYS. ACTA., 724 (1983), p 104.

REFERENCES (for Part II)

1. Chen Xiaoshu [7115 2556 2562], et al., SELENIUM IN BIOLOGY AND MEDICINE (Eds. Spallholz, J. E., et al.), 1980, pp 171-175.

2. Li Chongzheng [2621 1504 2973], et al., ZHONGHUA YIXUE ZAZHI [CHINESE MEDICAL JOURNAL], 3 (1979), p 169.

3. Schrauzer, G. N., SELENIUM IN BIOLOGY AND MEDICINE (Eds. Spallholz, J. E., et al.), 1980, pp 98-102.

4. Shamberger, R. J., BIOCHEMISTRY OF SELENIUM (Ed. Earl Frieden), Plenum Press, New York and London, 1983, pp 222-224.

5. Yang Fuyu, et al., ZHONGGUO KEXUE (B JI), 1986, 4: pp 396-400.

6. Polyacrylamide Gel Electrophoresis-Laboratory Techniques, PHARMACIA FINE CHEMICALS, 1983, p 25.

7. Nicolson, G. L., et al., J. CELL BIOL., 51 (1971), pp 265-272.

8. Ellman, G. L., et al., ARCH. BIOCHEM. BIOPHYS., 82 (1959), pp 70-77.

9. Hefeman, D. G., et al., J. NUTR., 104 (5) (1974), p 580.

10. Pearson, T. W., LIFE SCIENCES, 22 (1978), p 127.

11. Rotruck, J. T., et al., J. NUTR., 102 (1972), pp 689-696.

12. Mikuni-Takagaki, Y., et al., J BIOL. CHEM., 256 (1981), pp 8,463-8,469.

13. Underhill, C. B., et al., EXP. CELL RES., 131 (1981), pp 419-523.

14. Fosse, E. F., et al., BIOCHEM. BIOPHYS. ACTA, 649 (1981), p 507.

15. Morichesi, V. T., et al., J. MEMBRANE BIOL., 51 (1979), pp 101-131.

16. Steck, Th. L., et al., J. CELL BIOL., 62 (1974), pp 1-19.

17. Cogan, U., et al., BIOCHEM., 20 (1981), pp 6,396-6,403.

18. Henis, Y. I., et al., J. BIOL. CHEM., 257 (1982), pp 1,407-1,411.

19. Schachter, D., et al., BIOCHEM., 21 (1982), pp 2,146-2,150.

20. Siami, G., et al., J. NUTR., 102 (1972), pp 857-863.

21. Combs, G. F., et al., POULT. SCI., 54 (1975), pp 1,152-1,158.

22. Wu, S. H., et al., BIOL. REPROD., 20 (1973), pp 793-798.

23. Bielstein, M. A., et al., J. INORG. BIOCHEM., 15 (1981), pp 339-347.

24. Bielstein, M. A., et al., J. NUTR., 113 (1983), pp 2,138-2,146.

25. Lawrence, R. A., et al., ibid., 108 (1978), pp 211-215.

10,424/9599
CSO: 4009/1083

CRYSTAL AND MOLECULAR STRUCTURE OF TWO ISOMERS OF 2,3-DICYANO-2,3-DIPHENYL DIETHYLESTER SUCCINATE

Beijing ZHONGGUO KEXUE (B JI) [SCIENTIA SINICA: SERIES B (CHEMICAL, BIOLOGICAL, AGRICULTURAL, MEDICAL & EARTH SCIENCES)] in Chinese No 4, 1986 pp 337-344

[Article by Liu Youcheng [0491 2589 2052] and Yang Dilun [2799 4574 0243] of Department of Chemistry, Lanzhou University; and Yang Qingzhuan [2799 3237 0278], Han Wangzhen [7281 3769 4176], Shao Meicheng [6730 5019 2052] and Tang Youqi [0781 2589 4388] of Physical Chemistry Department, Beijing University]

[Abstract] 2,3-Dicyano-2,3-diphenyl diethylester succinate is made by oxidative coupling of a Cu^{++}-TMEDA-O_2 system with alpha-cyanoethyl phenyl acetate. Through column layer analysis of the product, two crystal compounds 1 and 2 are obtained. By X-ray analysis determination of the crystal structures of monocrystalline of compounds 1 and 2, they were found to be meso and racemic 2,3-dicyano-2,3-diphenyl diethylester succinate, respectively. It is noteworthy that there is an obvious stretching effect on the bond length of the central C-C single bond in molecules of compounds 1 and 2; in the former, it is 1.585 Å while in the latter-1.62 Å. In addition, there is apparent an steric hindrance effect between the substituent radicals linking carbon atoms at both ends of the central C-C bond. With these facts and the electronic effect of the substituent radicals in the molecules, this chemical compound breaks down readily into free radicals, thus providing an effective structural illustration of the polymerization of an initiator. Using the CNDO/2 method, the authors calculated the charge distribution and the Wiberg bond level of atoms in a molecule of compound 1. The result agrees quite closely with the crystal structure analytical results. Three figures show the shapes and bond length of compounds 1 and 2, as well as charge distribution and Wiberg bond level of compound 1. Four tables list the conditions under which crystallographic and diffraction-intensity data were gathered, some non-bond-connected interatomic distances, atomic coordinates, temperature factors, and bond angles. The first draft was received on 14 January 1984; the revised draft of the paper was received for publication on 22 June 1984.

REFERENCES

1. de Jongh, H. A., de Jonge, R. H. I., and Mijs, W. J., J. ORG. CHEM., 36 (1971), p 3,160.

2. ——— et al., MAKROMOL. CHEM., 157 (1972), p 279.

3. Liu Youcheng, Yang Dilun, and Lu Huilin [0712 1920 5259], GAODENG XUEXIAO HUAXUE XUEBAO [CHEMISTRY JOURNAL OF HIGHER SCHOOLS], 5 (1984), 3: p 410.

4. Allemand, J., and Gerdil, R., ACTA CRYSTALLOGRAPHICS, B34 (1978), p 2,214.

5. Szabo, Z. G., and Konkoly Thege, I., ACTA. CHIM. ACAD. SCI. HUNG., 86 (1975), 2: p 127.

6. Christoph Ruchardt and Hans-dieter Beckhaus, ANGEW. CHEM. INT. ED. ENGL., 19 (1980), p 437.

10,424/9599
CSO: 4009/1083

STUDIES OF ULTRAPURE TRIETHYLALUMINUM AND TRIETHYLGALLIUM

Shanghai HUAXUE SHIJIE [CHEMICAL WORLD] in Chinese No 7, 25 Jul 86
pp 292-295

[Article by Lu Fengzhen [7120 7685 6297] (since deceased), Ding Yongqing [0002 3057 1987], Wang Jiakuan [3769 0857 1401], Peng Ruiwu [1756 3843 0124] and Ren Yaocheng [0117 1031 2052] of Shanghai Institute of Metallurgy, Chinese Academy of Sciences; and Tu Jiahao [3205 0857 3185] and Zhang Xiqing [1728 6932 0615] of Shanghai Institute of Chemical Engineering]

[Abstract] Simplicity and effectiveness are guidelines in improving materials preparation with the ever-advancing semiconductor industry. Metalorganic chemical vapor deposition (MOCVD) has features of simple and flexible operation as well as low growth temperature, therefore MOCVD has become one of the most attractive new techniques for producing group III through group V compounds--semiconductor materials with new structures. The synthesis and purification of alkyl-radical metal compounds (a key material needed in MOCVD technique) are becoming new area of study. Thus, the authors studied purification based on distillation of the commercially available triethylaluminum to yield ultrapure triethylaluminum, as well as the direct synthesis and distillation purification of ultrapure triethylaluminum and gallium trichloride to yield ultrapure triethylgallium.

Under the identical distillation conditions, glass and quartz distillation columns were used to investigate the purification of triethylaluminum, as well as the purification of triethylgallium (using a quartz column) in collecting different rectification fractions (in percentage) of triethylgallium. The results are shown in the following Tables 1 and 2.

Table 1. Impurities in triethylamine.

(1)精馏柱	(2)实验号	(3) 杂质元素(ppm) K	Na	Ca	Mg	Zn	Cd	Cr	Fe	Si	Cu
(4)石英	RTEA-85-01	<0.28	<0.07	N.M	N.M	<0.28	<0.28	N.M	<1.18	<5.1	<0.17
	RTEA-85-02	<0.14	<0.05	N.M	N.M	<0.14	<0.14	N.M	<0.69	<5.1	<0.24
(5)玻璃	RTEA-84-01	<1.0	<1.0	N.M	<0.1	N.M	N.M	N.M	<1.0	<14	<3.0

Key:
1. Distillation column;
2. Experiment number;
3. Impurity element (ppm);
4. Quartz;
5. Glass.

Table 2. Impurities in triethylgallium

(1) 数据来源	TEG流出量(%)	(2) (3) 杂质元素(ppm) K	Na	Ca	Mg	Zn	Cd	Cr	Fe	Si	Cu
(4) 本文 RTEG-84-01	~30	<1.4	<1.4	N.M	<0.7	<0.14	<0.21	N.M	<0.7	<14	<3.0
(5) 本文 RTEG-85-02	~70	0.68	16	N.M	0.7	<0.4	<0.8	N.M	38	5.0	<0.6
(6) 日本 Sumitomo Chem.Co.		N.M	N.M	<0.05	0.1	0.2	0.1	0.1	2.0	87	N.M

Key:
1. Source of data;
2. Outflow of TEG (in percent);
3. Impurity element (ppm);
4. This paper (ETEG-84-01);
5. This paper (RTEG-85-02);
6. Sumitomo Chemical Co. of Japan

Two figures show the arrangement for preparing ultrapure triethylaluminum and triethylgallium, and a fluorescence diagram of the spectral line of the MOCVD-GaAs extension layer.

REFERENCES

[1] K.L. Hess, P.D. Dapkus et al., J. of Electronic Materials 11(6), 1115~1137 (1982).

[2] Lu Fengzhen et al., XIYOU JINSHU [RARE METALS] (Foreign Edition), 4 (4), 1~8 (1985).

[3] Ding Yongqing et al., SHANGHAI JINSHU [SHANGHAI METAL), (4), 1~4 (1985).

10424/9835
CSO: 4009/1110

CSR-8401 EXPANDED-RANGE RESISTANCE PROBE INSTRUMENT

Shanghai DIANZI YU ZIDONGHUA [ELECTRONICS AND AUTOMATION] in Chinese No 1, 20 Feb 86 pp 1-4, 38

[Article by Zhang Jinghai [1728 2417 3189], Bao Zongming [0545 1350 2494] and Shu Chang [5289 2545] of Fudan University; and Zhou Xinde [0719 0207 1795], Xia Zhiliang [1115 1807 5328], Lin Xianqi [2651 0341 7871], Hou Rifa [0186 2480 4099] and Hu Jihong [5170 4949 1347] of Shanghai Institute of Technical Physics, Chinese Academy of Sciences] [Abstract] Fudan University and Shanghai Institute of Technical Physics jointly developed the CSR-8401 expanded-range resistance probe instrument (with five subassemblies: probe system, sample stand, moving system, control system, and printing-drawing system). On-line data processing can be conducted by interfacing with an Apple-II microcomputer; alternatively, the probe system can operate independently without a microcomputer. The functions of the probe instrument expanded-range test resistance, and internal repetition standard correspond to instruction-manual indexes of ASR series products (made in the United States), which are unique in the international market. The CSR-8401 instrument is expected to be available commercially in 1985. The instrument has the four following indexes: (1) reproducibility accuracy--better than 1 percent; (2) measurement range--from 1 to 10^8 ohms; (3) discriminability of measurement depth--300 A; and (4) moving accuracy of sample stand 50 um$\pm$5 percent. One table shows the operation of each step of the main controller for controlling the measurement procedures of the probe instrument. Eleven figures show the CSR-8401 main components, current lines and potential distribution in a semiconductor, profile of the CSR-8401, components of control and measurement system, flow chart of control process, X-Y feed system, principles of constant and varying current, as well as drawing layout; and measurement results in plotted curves.

10424/9190
CSO: 4009/1095

Microbiology

PURIFICATION AND PARTIAL CHARACTERIZATION OF ENTEROTOXINS C_1, C_2 PRODUCED BY STAPHYLOCOCCUS AUREUS STRAINS 137,361

Beijing WEISHENGWUXUE TONGBAO [MICROBIOLOGY] in Chinese Vol 13, No 3, Jun 86 pp 113-116

[Article by Lei Zuorong [7191 2683 2837], Qu Liyun [2575 7787 0061] and Wang Luming [3769 7627 2494] of Institute of Epidemic Microbiosis, Academy of Military Medical Sciences, Beijing]

[Abstract] From a crude enterotoxin solution of Staphylococcus aureus, the authors extracted enterotoxin C_1; its 90 percent purity was accomplished by using only a one-layer analysis of a CM-fibrin column. Enterotoxin C_2 was extracted in two steps: Cm-fibrin column (step-by-step elution)→ Sephadex G-75, and filtration, achieving 98 percent pure enterotoxin C_2. The recovery rate of enterotoxin is 66 percent in the CM-fibrin layer analysis; the recovery rate is similar to that in experiments by Avena et al. Using enterotoxin C_1, C_2 (purity more than 90 percent) as immunogen--injected into a group of domestic rabbits, high-efficacy antiserums C_1, C_2 were obtained. The precipitation curves of these serums with the authors' antigens C_1, C_2 were compared with the precipitation curve of the reference standard antigens; the peaks of these curves match each other.

One table lists the purification recovery rates of enterotoxin C_2 produced by Staphylococcus aureus. Five figures show layer analysis spectrograms of a CM-fibrin column with enterotoxin C_1 and a layer analysis spectrogram (using Sephadex G-75) to purify enterotoxin C_2, and circular-disk electrophoresis determinations using polypropene acylamine on enterotoxin C_1 and C_2 produced by Staphylococcus aureus. The authors of Military Medical Sciences, for the determination of equipotential points.

REFERENCES

[1] Borja, C.R. et al.: BIOCHEM. 6: 1467, 1967.

[2] Avena, R.M. et al.: BIOCHEM. 6: 1474, 1967.

[3] Robern, H. et al.: BIOCHEM. BIOPHYS. ACTA. 393: 148, 1975.

[4] Shinagawa, K. et al.: JAP. J. BACTERIOL, 30: 683, 1975.

[5] Yao Zhongxi [1202 1813 4406] et al., ZHONGHUA WEISHENGWUXUE JI MIANYIXUE ZAZHI [CHINA JOURNAL OF MICROBIOLOGY AND IMMUNOLOGY], 3 (5): 334, 1983.

[6] Weir, D.M.: Handbook of Experimental Immunology. Second Edition 2.9-2.11, Blackwell Scientific Publication Oxford/Loudon/Edinburgh/Melbourne, 1973.

[7] Shinagawa, K. et al.: JAP. J BACTERIOL. 30: 683, 1975.

10424/9835
CSO: 4009/1006

METHOD OF CYMEGESOLATE ON INDUCTION OF SISTER CHROMATID EXCHANGE OF BONE MARROW CELL IN MICE

Beijing YAOXUE TONGBAO [CHINESE PHARMACEUTICAL BULLETIN] in Chinese Vol 21, No 8, 8 Aug 86 pp 451-452

[Article by Wang Renli [3769 0088 4409], Ding Yinuo [0002 0076 6179] and Zhang Zhongshu [1728 1813 1859] of Shanghai Municipal Institute of Planned Parenthood Science]

[Abstract] After injections of 5-iodo-2'-deoxy-urea pyrimidine nucleotide (IfUrd)--activated carbon suspension fluid in the abdominal cavity of mice (five groups): cymegesolate (in doses of 15, 75 and 375 mg/kg), cyclophosphoacylamine and control groups, chromatids of bone marrow cell were prepared and sister chromatid exchange rates (SCE) were observed. Compared to the control group, a cymegesolate dose of 15 mg/kg had no effect on the SCE frequency of mouse bone-marrow cells. The SCE frequencies for 75 and 375 mg/kg cymegesolate doses were, respectively, 1.35 $\pm$ 0.12/cell (bone marrow) and 5.10 $\pm$ 0.44/cell (bone marrow). The differences are significant compared to the control group.

The compound cymegesolate is a contraceptive with relatively few side reactions. However, whether or not long-term administration of this contraceptive will lead to a potential health risk remains to be answered by research. This paper reports these studies. A table lists data comparing SCE frequencies of bone marrow cells in the five mouse groups.

Although the particular doses described in the paper did not induce any degeneration in mice given the contraceptive, it remains to be seen whether any higher doses will make a difference. Further studies are necessary to comprehensively evaluate the hereditary safety of cymegesolate.

REFERENCES

1. Zhang Zhongshu et al., SHENGZHI YU BIYUN [CONCEPTION AND CONTRAC%PTION], 1982; 2 (1):37.

2. Zheng Huizhen [6774 1979 3791] et al., SHENGZHI YU BIYUN, 1983: 3 (2): 39.

3. Kanda N et al., EXPERIMENTAL CELL RESEARCH 1979: 118:431.

4. Ramirez P M, MUTATION RESEARCH 1980: 74:61.

5. Wang Renli, et al., YIZHANG [HEREDITY], 1984: 3:11.

6. Zheng Huizhen et al., YIZHANG YU JIBING [HEREDITY AND DISEASE], 1984: Vol. 1, No 1 (inauguration issue), 21.

7. Chen Huiling [7115 5610 3781] et al., SHENGWU HUAXUE YU SHENGWU WULI XUEBAO [JOURNAL OF BIOCHEMISTRY AND BIOPHYSICS], 1981: 13 (2):125.

8. WHO Tech Rep Ser No 563, 1975: 34.

APPLICATION OF MANNITOL IN EARLY BURN STAGE

Beijing YAOXUE TONGBAO [CHINESE PHARMACEUTICAL BULLETIN] in Chinese Vol 21, No 8, 8 Aug 86 pp 464-466

[Article by Lei Wanjun [7191 5502 6511], Burn Injury Ward, Hospital of Loyang Medical College]

[Abstract] Mannitol is a diuretic; its administration in the early stage of burn injury can improve the redistribution of body fluids, relieve tissue edema, expand blood vessels in the kidneys, and increase urination for the elimination of harmful substances. So the application of mannitol in the early stage after a burn injury tends to assist in surviving the shock period and preventing (and treating) complications of internal organs. The paper presents the author's experience in clinical treatment with mannitol in the early period after burn injuries; effects on shock treatment, renal and pulmonary functions, and precautions in the intravenous-drip administration of mannitol.

REFERENCES

1. Lei Wenjun et al., JICENG YIKAN [MEDICAL JOURNAL ON FUNDAMENTALS], 1982: 2 (6): 11.

2. Chen Minzhang [7115 2404 4545] et al., LINCHUANG SHUI DU DIANJIEZHI PINGHENG [EQUILIBRIUM BETWEEN WATER AND ELECTROLYTE IN CLINICAL PRACTICE], People Sanitation Publishing House, 1981: 247.

3. Xie Baizhang [6200 2672 2874] et al., WAIKE BINGREN DI NEIKE CHULI [INTERNAL-MEDICINE THERAPY ON INJURED PATIENTS], Jiangsu Science and Technology Publishing House, 1982; 121.

4. (compiled by) Huang Senlin [7806 2773 2651], SHAOSHANG [BURN INJURY], supplementary edition, 1975: 69:182.

5. Pan Shicheng [3382 0013 1361] et al., XIUKE [SHOCK], People Sanitation Publishing House, 1982:260.

6. Selected Papers at Burn Injury Prevention and Treatment Symposium of the PRC Liberation Army, 1979: 343.

7. (chief editor) Zhu Yan [2612 8746], XIUKE DI LINCHUANG [CLINICAL PRACTICE ON SHOCK], Zhejiang Science and Technology Publishing House, 1982: 243.

8. First Hospital, Zhejiang Medical University, JIXING SHENGONGNENG SJUAIJIE [ACUTE RENAL INSUFFICIENCY], Shanghai People Publishing House, 1976: 37.

9. (chief editors) WENG WEIQUAN [5040 4850 2938] et al., NEIKE WEIZHONGZHENG DI QIANGJIU [FIRST AID ON SEVERE, CRITICAL INTERNAL DISEASES], People Sanitation Publishing House, 1985: 590.

10424/12859
CSO: 4009/1111

Physics

USES OF AMORPHOUS ALLOYS IN CHINA

Beijing WULI [PHYSICS] in Chinese Vol 15 No 6, Jun 86 pp 355-360

[Article by Zhang Luo [1728 3157], Liu Guangdi [0491 0342 2769], Shi Songyue [4258 2646 6460] and Meng Jiandong [1322 1696 2767] of Shanghai Institute of Iron and Steel]

[Abstract] It was estimated that 5 to 10 tons of amorphous band-shaped alloys would be supplied to China's domestic users from domestic sources to manufacture electronic or electrical products; some products were sold in domestic and international markets, while others were used in Chinese defense projects. The paper presents the following applications of amorphous alloys made with rapid quenching: leakage switches, power source of switches, pulse transformers, power transformers, transducers, magnetic heads, magnetic shields, magnetic separation, and soldering components, among other applications. Researchers contributing to the development are named.

Four figures show the operating principle of a leakage switch, temperature rise curves of amorphous and Si-Fe transformers, magnetic properties of transformers, and the wear-resistance service life of amorphous and permalloy magnetic heads. Seven tables list data on technical parameters of the power source for a 5 kW switch, comparison of power sources for amorphous and ferrite 20 kHz pulse coding modulation switches, magnetic properties of transformers, performance comparison of transformers made of different materials, properties of amorphous pressure transducers, comparison of frequency response characteristics in loudspeakers linked to several stereosonic magnetic heads, and the quality and economic benefits of soldering using tin and versus using electric resistance.

10,424/9599
CSO: 4009/109

MILLIMETER-WAVE SCATTERING SYSTEM FOR PLASMA DIAGNOSTICS

Beijing WULI [PHYSICS] in Chinese Vol 15 No 6, Jun 86 pp 365-366, 384

[Article by Cui Binsheng [1508 3453 3932], Wu Xiaowen [0702 1420 2429], Yu Xuehua [0205 7185 5478], and Yuan Dingpu [5913 1353 2883] of Institute of Physics, Chinese Academy of Sciences; and Kuang Longhai [0562 7893 3189] of Institute of Electronics, Chinese Academy of Sciences]

[Abstract] The millimeter-wave scattering system is one among the important diagnostics methods for studying the plasma collective effect owing to the characteristics of high scattering power and large scattering angle. The development of this scattering system is an important sector in experiments since the system is responsible for success or failure in experiments. The paper discusses the scattering system, including its operating principle, adaptation conditions, heterodyne mixing frequency system, and zero-beat mixing frequency scattering system. The following diagram shows the operating principle of the scattering system:

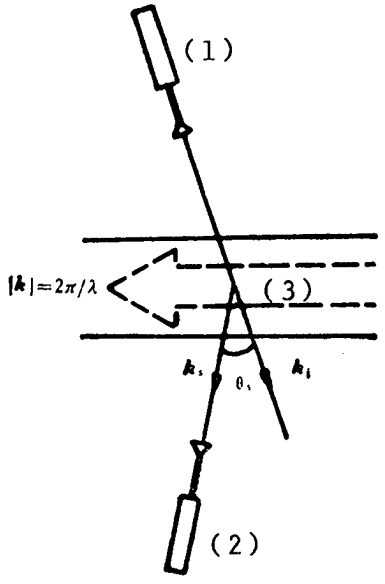

Key:
1. Transmitter
2. Receiver
3. Plasma low-frequency wave

Two other figures show the heterodyne mixing frequency system, zero-beat mixing frequency scattering system, and frequency spectrum of the scattering signal with a 10° scattering angle. Both the heterodyne and zero-beat mixing frequency systems can be used for diagnosing low-temperature, high-density fluctuation plasma in its low frequency band and its instability. The heterodyne system is adapted to conditions of large scattering angle and high frequency, while the zero-beat system is adapted to low frequencies. The authors are grateful to Chen Chunguang [7115 2504 0342] and Yang Size [2799 1835 3419] for their direction; and Yu Changxuan [0205 2490 2467] for his assistance.

10,424/9599
CSO: 4009/109

END